



2017

# A PORTABLE SENSOR FOR MEASURING GAS EMISSIONS FROM DAIRY COMPOST BEDDED PACK BARNS

Katharine Wolf

*University of Kentucky*, [katharine.wolf@uky.edu](mailto:katharine.wolf@uky.edu)

Digital Object Identifier: <https://doi.org/10.13023/ETD.2017.393>

**[Click here to let us know how access to this document benefits you.](#)**

---

## Recommended Citation

Wolf, Katharine, "A PORTABLE SENSOR FOR MEASURING GAS EMISSIONS FROM DAIRY COMPOST BEDDED PACK BARNS" (2017). *Theses and Dissertations--Biosystems and Agricultural Engineering*. 51.  
[https://uknowledge.uky.edu/bae\\_etds/51](https://uknowledge.uky.edu/bae_etds/51)

This Master's Thesis is brought to you for free and open access by the Biosystems and Agricultural Engineering at UKnowledge. It has been accepted for inclusion in *Theses and Dissertations--Biosystems and Agricultural Engineering* by an authorized administrator of UKnowledge. For more information, please contact [UKnowledge@lsv.uky.edu](mailto:UKnowledge@lsv.uky.edu).

**STUDENT AGREEMENT:**

I represent that my thesis or dissertation and abstract are my original work. Proper attribution has been given to all outside sources. I understand that I am solely responsible for obtaining any needed copyright permissions. I have obtained needed written permission statement(s) from the owner(s) of each third-party copyrighted matter to be included in my work, allowing electronic distribution (if such use is not permitted by the fair use doctrine) which will be submitted to UKnowledge as Additional File.

I hereby grant to The University of Kentucky and its agents the irrevocable, non-exclusive, and royalty-free license to archive and make accessible my work in whole or in part in all forms of media, now or hereafter known. I agree that the document mentioned above may be made available immediately for worldwide access unless an embargo applies.

I retain all other ownership rights to the copyright of my work. I also retain the right to use in future works (such as articles or books) all or part of my work. I understand that I am free to register the copyright to my work.

**REVIEW, APPROVAL AND ACCEPTANCE**

The document mentioned above has been reviewed and accepted by the student's advisor, on behalf of the advisory committee, and by the Director of Graduate Studies (DGS), on behalf of the program; we verify that this is the final, approved version of the student's thesis including all changes required by the advisory committee. The undersigned agree to abide by the statements above.

Katharine Wolf, Student

Dr. Michael Sama, Major Professor

Dr. Donald Colliver, Director of Graduate Studies

---

A PORTABLE SENSOR FOR MEASURING GAS EMISSIONS FROM DAIRY COMPOST  
BEDDED PACK BARNs

---

THESIS

---

A thesis submitted in partial fulfillment of the requirements for the degree of  
Master of Science in Biosystems and Agricultural Engineering in the  
College of Engineering at the University of Kentucky

By

Katharine Wolf

Lexington, Kentucky

Co-Directors: Dr. Michael Sama & Dr. Joseph Taraba

Professors of Biosystems & Agricultural Engineering

Lexington, Kentucky

Copyright © Katharine Wolf 2017

## ABSTRACT OF THESIS

### A PORTABLE SENSOR FOR MEASURING GAS EMISSIONS FROM DAIRY COMPOST BEDDED PACK BARNs

The objective of this study was to develop a gas measurement chamber for the comparison of emissions from different dairy manure storage facilities. Compost bedded pack (CBP) barns are a loose housing system in which cows rest on an intensely managed compost pack. Sawdust is the primary material added to the system, along with manure and urine inputs from the cows, and the pack is stirred one to two times daily. Maintaining a high level of aerobic microbial activity in the pack is critical for cow health. Previous dairy emissions work has not included compost bedded pack barns; it was expected that the largely aerobic tilled layer of the system would have a different emissions profile than other manure storage systems. A measurement chamber was developed to determine emission fluxes from the compost bedded pack barn surface. Infrared and electrochemical sensors measuring ammonia, methane, and carbon dioxide obtain headspace gas concentrations, temperature, and humidity each second. The relatively lower cost of each chamber, as compared to photoacoustic and gas chromatography systems, will allow a greater number to be deployed to more accurately represent the spatial variation within the system.

**KEYWORDS:** Compost bedded pack barns, compost bedded dairy pack barns, greenhouse gas, measurement chamber, portable gas sensor

---

Katharine M. Wolf

---

July 27, 2017

A PORTABLE SENSOR FOR MEASURING GAS EMISSIONS FROM DAIRY COMPOST  
BEDDED PACK BARNs

By

Katharine M. Wolf

Dr. Michael Sama

---

(Co-Director of Thesis)

Dr. Joseph Taraba

---

(Co-Director of Thesis)

Dr. Donald Colliver

---

(Director of Graduate Studies)

July 27, 2017

---

(Date)

## TABLE OF CONTENTS

TABLE OF CONTENTS .....	iii
LIST OF FIGURES.....	v
LIST OF TABLES .....	vi
TABLE OF EQUATIONS.....	vii
CHAPTER 1: LITERATURE REVIEW.....	1
1.1. Introduction .....	1
1.2. Compost bedded pack barns.....	1
1.2.1. Basic composting process .....	2
1.2.2. Weather controls .....	7
1.2.3. Producer controls.....	9
1.2.4. Influence of CBP on cows.....	13
1.2.5. Summary .....	14
1.3. General dairy emissions.....	15
1.3.1. Introduction .....	15
1.3.2. Overview of GHG processes.....	16
1.3.3. Potential control points for dairy GHGs .....	17
1.3.4. Summary .....	19
1.4. Chamber design to measure GHG emission.....	20
1.4.1. Background .....	20
1.4.2. Application to the compost bedded pack barn .....	24
1.5. Objectives .....	27
CHAPTER 2: Prototype Emissions Measurement Chamber .....	28
2.1. Introduction .....	28
2.2. Materials and Methods .....	28
2.2.1. Infrared sensor.....	29
2.2.2. Electrochemical sensor.....	31
2.2.3. Programming.....	32
2.3. Results and Discussion.....	35
2.4. Conclusions .....	36
CHAPTER 3: Emissions Measurement Chamber Calibration.....	37
3.1. Introduction .....	37
3.2. Materials and Methods .....	37
3.2.1. Calibration gases .....	37
3.2.2. Individual sensor calibration.....	37
3.2.3. Chamber calibration .....	39
3.2.4. Temperature and humidity .....	39
3.3. Results and Discussion.....	40
3.4. Conclusions .....	46
CHAPTER 4: Preliminary CBP Barn Emissions Measurement .....	47
4.1. Introduction .....	47
4.2. Materials and Methods .....	47
4.3. Results and Discussion.....	49

4.3.1. June 15 collection.....	51
4.3.2. June 21 collection.....	52
4.3.3. June 29 collection.....	53
4.3.4. July 6 collection .....	55
4.3.5. Analysis of initial slopes .....	58
4.4. Conclusions .....	62
CHAPTER 5: Conclusions.....	63
APPENDICES.....	67
Appendix A. drycalcs.m MATLAB script for evaluating drying characteristics of particles. .....	67
Appendix B. ChamberMeasIR VB.net program for data collection. ....	76
Appendix C. Supplementary program for use during calibration to write values to the evaluation boards.....	80
Appendix D. chambhum.m MATLAB script to evaluate time to excessive humidity in chamber. ....	81
Appendix E. ssfind.m MATLAB script to find steady-state values for IR sensor calibration. .....	83
Appendix F. ssfinddec.m MATLAB script to find steady-state values for electrochemical sensor calibration.....	86
Appendix G. ssoptions.m MATLAB script for deciding most effective choice of average and error to use for finding steady-state value for sensor calibration. ....	87
Appendix H. slopefind.m MATLAB script for original attempts at fitting a curve to the IR CO <sub>2</sub> data and calculating initial emission rate.....	88
BIBLIOGRAPHY .....	89
VITA .....	93

## LIST OF FIGURES

Figure 1-1. Overview of the basic composting process in a CBP. ....	2
Figure 1-2. Weather influence on the overall composting process in a CBP. ....	7
Figure 1-3. Interaction of weather controls and producer controls with the composting environment in a CBP. ....	9
Figure 1-4. Diagram of the relationships between processes within the compost bedded pack barn environment and their impact on cow health and productivity. ....	13
Figure 2-1. First tab of SGX software. ....	30
Figure 2-2. Voltage adjustment tab of SGX software. ....	31
Figure 2-3. Program developed for data collection. ....	33
Figure 2-4. Chamber prototype consisting of a mixing bowl, with sensors inserted in the top. ....	35
Figure 3-1. Close-up of individual sensor calibration process. ....	38
Figure 3-2. Sensors were calibrated in a fume hood while the program ran on a tablet PC. ....	39
Figure 3-3. Predicted vs actual CH <sub>4</sub> concentration as generated from the two-point calibration. ....	43
Figure 3-4. Predicted vs actual CO <sub>2</sub> concentration as generated from the two-point calibration. ....	44
Figure 3-5. Predicted vs actual NH <sub>3</sub> concentration as generated by the two-point calibration. ....	45
Figure 3-6. Chamber purge with CO <sub>2</sub> . ....	46
Figure 4-1. Collection setup with the chamber in the CBP. ....	49
Figure 4-2. June 15 IR and GC measurements. ....	51
Figure 4-3. June 21 GC and IR data for all gases. ....	52
Figure 4-4. June 29 CO <sub>2</sub> data from IR sensor. ....	54
Figure 4-5. June 29 humidity buildup. ....	55
Figure 4-6. July 6 CO <sub>2</sub> from both IR and GC, all deployments. ....	56
Figure 4-7. July 6 CH <sub>4</sub> from GC. ....	57
Figure 4-8. July 6 N <sub>2</sub> O from GC. ....	58
Figure 5-1. Example layout of chambers for sampling entire barn. ....	64



## LIST OF TABLES

Table 3-1. Prediction intervals for calibrated gas sensors. ....	43
Table 4-1. Summary of sampling schemes. ....	48
Table 4-2. Compost temperature (°C) near the measurement point at various depths. ....	53
Table 4-3. Comparison of initial slopes of potential concentration curves obtained via IR and GC (ppm/sec) on June 21. ....	60
Table 4-4. Gas analysis via GC on June 21. ....	61
Table 4-5. Summary of calculated emission rates. ....	61
Table 5-1. Comparison of emissions across several studies. ....	66

## TABLE OF EQUATIONS

Equation 1-1.....	16
Equation 1-2.....	16
Equation 1-3.....	17
Equation 2-1.....	33
Equation 3-1.....	40
Equation 3-2.....	40
Equation 3-3.....	40
Equation 3-4.....	41
Equation 3-5.....	41
Equation 3-6.....	41
Equation 3-7.....	42
Equation 3-8.....	42
Equation 4-1.....	59

## CHAPTER 1: LITERATURE REVIEW

### 1.1. Introduction

Compost bedded pack barns (CBP) are a relatively new but increasingly popular dairy housing option (Black et al. 2013), offering potential advantages in cow comfort compared to freestall systems. The intensive management required makes CBP particularly well-suited for small farms, such as the 88-cow Kentucky herd average (Kentucky Farm Bureau, 2015). Field studies with dairy compost have shown some benefits in application to agricultural soil. Amon et al. (2001) detected no NH<sub>3</sub> emissions after spreading composted dairy manure, compared to stack manure in which most NH<sub>3</sub> emissions occurred after spreading. Hammond (2015) found that compost from a CBP provided more plant-available P than fresh manure, and with similar decomposition characteristics to fresh manure. However, there is still a need to evaluate greenhouse gas (GHG) emissions from well-managed CBP systems. The US dairy industry has set a goal of a 25% reduction of the industry's GHG footprint by the year 2020 relative to 2009 (Innovation Center for US Dairy; <http://www.usdairy.com/sustainability/community-commitment/about>). Several attributes of the CBP show potential for contributing to this goal, and research toward that end could provide farmers with additional information when making dairy housing decisions.

### 1.2. Compost bedded pack barns

Compost bedded pack barns were developed by farmers mostly for their advantage in cow comfort. In an observational study of 42 farms with CBPs across KY, farmers reported their lactating cows had decreased lameness, decreased somatic cell

count (SCC), and decreased days open. Economically, CBPs are cheaper to construct than other options, but they do include constant input of more bedding resulting in more variable annual input costs (Black et al., 2013).

### 1.2.1. Basic composting process

Success of the CBP relies on managing the pack itself; composting depends on activity of bacteria and fungi to process raw materials, with fungi representing the largest fraction of the microbial biomass. The interaction between the most basic variables is diagrammed in Figure 1-1.

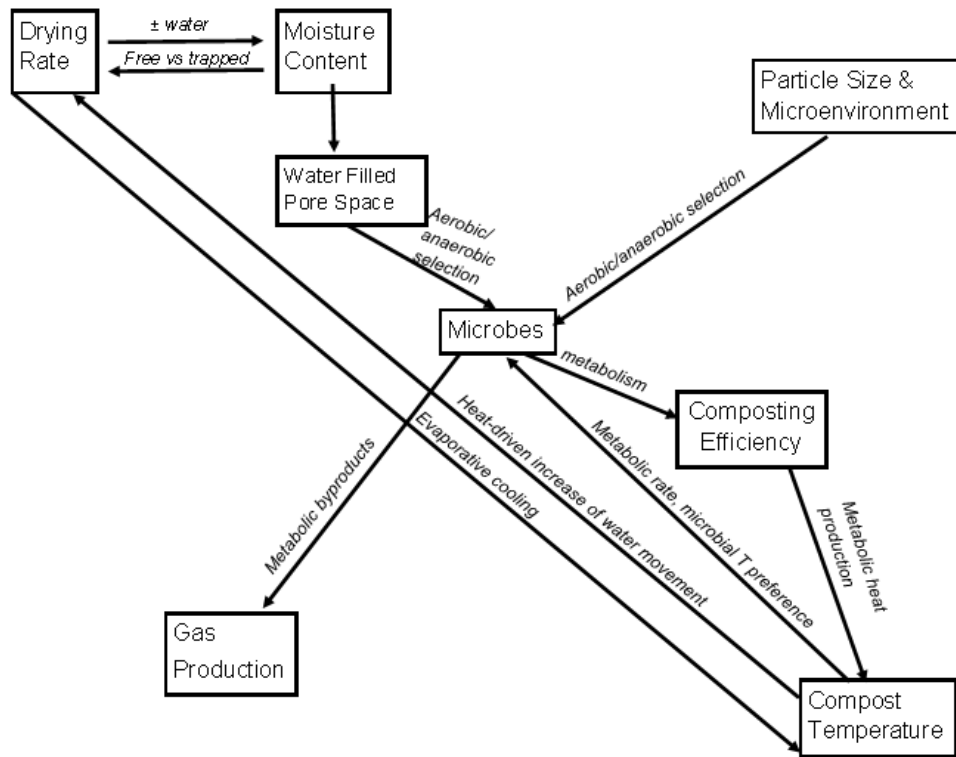


Figure 1-1. Overview of the basic composting process in a CBP.

The most central variable is moisture content (MC) because it directly influences mastitis risks and can quickly be changed by the producer; compost temperature, while frequently used to indicate composting success, is a lagging variable. A change in compost temperature follows other changes within the pack, so monitoring primarily MC should help producers catch issues more quickly than temperature alone, allowing them to alter management strategies before pack performance decreases substantially.

Moisture content has a two-way interaction with drying rate. First, it is obvious from the basic principles of mass transfer that an increased drying rate will reduce MC if no other factors are acting. However, it is important to note that MC also influences drying rate.

Two processes occur as porous systems dry (Mujumdar & Menon, 1995). The first is energy transfer from the environment in the form of heat; this process is a function of external conditions, especially temperature, relative humidity, air flow, surface area, and pressure. This is especially important for unbound surface moisture. The second process is mass transfer as internal moisture is moved to the solid surface, at which point the heat transfer process dominates those water particles. Water movement to the surface is primarily a function of internal conditions, especially the physical nature of the solid, temperature, and MC.

The two processes and their interaction can be seen by plotting drying rate versus MC of the system under observation. Three main stages exist (Mujumdar & Menon, 1995). First a constant drying rate exists while the surface has free moisture; the rate controlling step is diffusion of water vapor across the air-moisture interface, and the rate of the diffusion surface removal. Toward the end of this stage, moisture is transported

from inside the solid by capillary forces, though the rate may still be constant; the average MC then hits the critical MC, at which point the surface film has been so removed that dry spots appear on the surface. The second stage is the first falling rate period, in which the unsaturated surface dries until the surface is completely evaporated. The third stage is the second falling period, in which the controlling step is the rate at which moisture can move through the solid as a result of concentration gradients from interior to exterior surfaces. In G. Maia et al.'s (2012) work with a compost biofilter, a sharp transition was observed to be the critical point between 39-43% MC (wet basis).

Moisture content across the aggregate may then have a crucial effect on the presence of organisms. Mixed anoxic zones potentially promote denitrification internally. Maia et al. (2012) also examined microbial gas generation and removal throughout the drying process. Nitrogen biological transformations in nitrifying compost biofilters were affected by moisture similarly to soils. Methane generation started at the beginning of the falling drying rate, peaked during the falling drying rate where  $N_2O$  generation stopped, and ceased in the stable-dry system stage. This characteristic may be partially due to not only methanotroph activity, but also  $NH_3$  oxidizers oxidizing  $CH_4$  (Sylvia et al., 2005). Media moisture conditions potentially impact the removal and fate of contaminants in nitrifying gas-phase compost biofilters (Maia et al., 2012). Thus, any empirical observations of a compost system should be accompanied by MC measurements to be of use.

Willits (1974) combined heat and mass transfer equations to derive a model for parameters including drying time and the location of the drying front in poultry manure. The model evaluated spheres and cylinders considering multiple known parameters of the

environment and particle, with an empirical coefficient included. Willits considered the system dry at the equilibrium moisture. The equations are simple to both solve and model within mathematics software. Sexstone et al. (1985) modeled the oxygen distribution in a cross section of a particle with contour curves; a similar but more graphically advanced approach could be applied to drying front movement.

Moisture content is a contributing factor to water filled pore space (WFPS); at higher MC, pore space is more likely to be occupied by water than by air, influencing microbial activity. While water is necessary as a means for transport, WFPS greater than 60% increases the activities of microbes capable of using alternative electron acceptors, such as anaerobic denitrifiers (Paul, 2014). An excessively high MC may contribute toward selecting more anaerobic microbes; aerobic metabolism is generally more efficient in breaking down material and results in better heat generation. Shane et al. (2010) suggested MC be kept below 65% in the CBP; this was later tightened by Black et al. (2013) with a recommended optimal MC range of 45-55%.

In addition to simply MC, aggregate structure has significant effects on water movement and thus drying in soil, and this principle is also applicable in compost systems. Even in a generally well-aerated system, anaerobic microsites, influenced by intra-aggregate pore size, can exist within aggregates. Micropores will be more likely to restrict water movement due to capillary forces acting. Whether capillary flow outward occurs depends on the difference of the relative attraction between liquid-liquid molecules and liquid-solid molecules. Liquid is also held more tightly held at lower MC in porous solids (Wang et al., 2007). Overall, the heterogeneity of the composting environment makes it possible for the simultaneous occurrence of aerobic and anaerobic

processes, resulting in variation in gas production, which will be outlined more thoroughly in a later section.

Organisms produce heat as a result of metabolic processes. This heat results in an increase in compost temperature, which in turn can drive metabolic rate; such temperature-based changes are expressed as  $Q_{10}$  (Paul, 2014). Further, the microbial-driven changes in temperature may result in a selection pressure on the microbial population due to a variation in temperature preferences; a warmer environment will select for thermophiles, while a colder environment will select for psychrophiles, although the surface layer of compost is typically within the mesophilic temperature range. The CBP system is defined as “semi-composting” because it does not reach temperatures sufficient for material sanitization (Black, 2013). Because stirring is required to maintain the aerobic microbial population, it is critical that producers stir the pack consistently throughout the year, despite the perceived risk of decreasing pack temperature by introducing cold air in the winter. A two-way relationship also exists between compost temperature and drying rate because drying increases evaporative cooling (reducing pack temperature), while a higher compost temperature increases the drying rate.



1.2.2. Weather controls

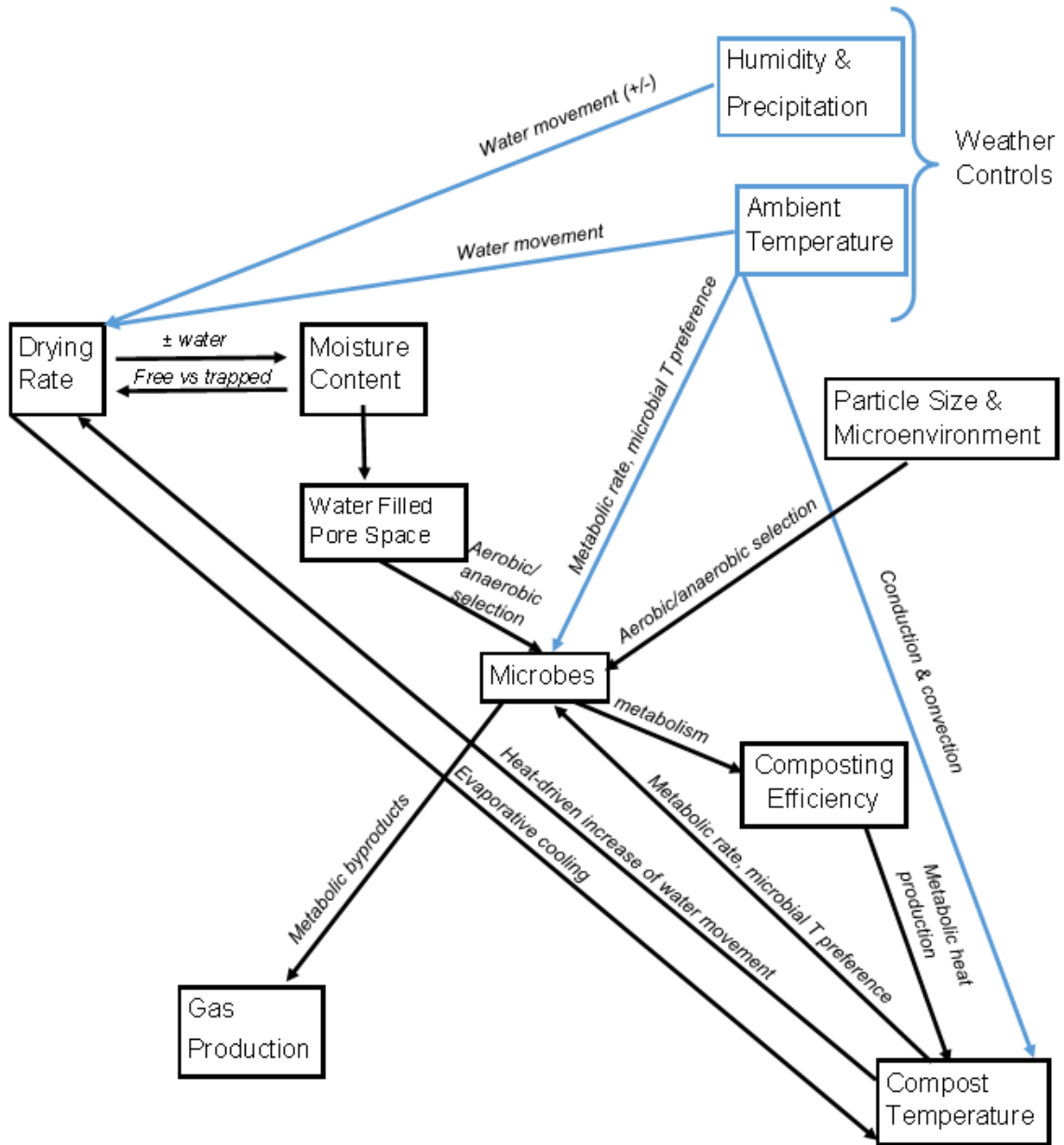


Figure 1-2. Weather influence on the overall composting process in a CBP.

Figure 1-2 outlines how weather influences the basic composting processes through changes in humidity, precipitation, and temperature. Precipitation can directly add moisture to the pack, especially influencing edges if curtains or some other physical barrier does not inhibit its movement into the barn. Humidity influences drying rate

because it determines the air's ability to pick up moisture; at higher humidity, lower drying rates can be expected, while the reverse is true of lower humidity assuming similar temperatures. Ambient temperature also influences drying rate because warmer air, in general, can contain more water than cooler air at 100% relative humidity. Microbial activity is impacted not only by selection pressure applied by ambient temperature, but also by changing metabolic rate, in an identical process to that previously discussed with compost temperature. Further, ambient temperature influences compost temperature via conduction and convection, in addition to indirectly through its influence on drying rate. Black (2013) described the effect of evaporation overcooling the pack in the winter, but not in the summer; Eckelkamp et al. (2016) observed that fluctuations in compost temperature followed those of ambient temperature throughout the year.

### 1.2.3. Producer controls

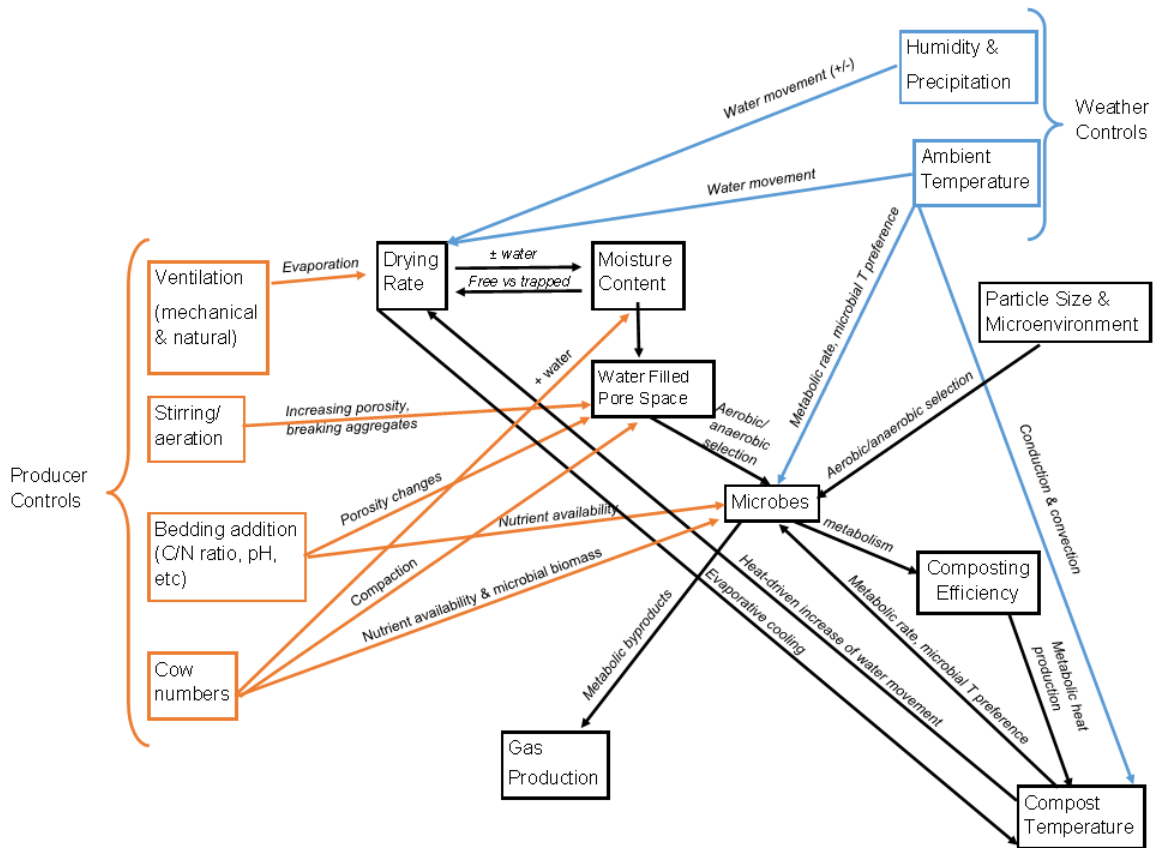


Figure 1-3. Interaction of weather controls and producer controls with the composting environment in a CBP.

While not directly depicted, the interaction of all three primary weather controls (precipitation, humidity, and temperature) should be a driver for producer controls. Producers ultimately control ventilation, pack aeration, bedding addition, and cow numbers (Figure 1-3). Black et al. (2013) described short-term and long-term factors influencing the compost bed, with short-term factors influencing the barn over the course of days to weeks and including weather, stocking density, pasture access, bedding, and stirring strategy; long-term factors include barn structure, air movement, curtains, and

manager knowledge. These previously described factors mostly fit well into the diagram in Figure 1-3.

Ventilation is necessary in any animal housing system and is especially a focus for cow cooling because a temperature-humidity index (THI) exceeding the cow's thermoneutral zone results in production losses. Humid environments such as Kentucky require even greater attention to air movement at the cow level; Berman (2005) noted that negative effects caused by increased humidity could be mitigated by maintaining air velocity of 1.5 to 2 m/s. In the CBP barn, ventilation is especially critical as it not only influences cows directly, but is necessary for pack drying; a higher air movement velocities results in a higher drying rate. Ventilation can be both natural and mechanical, with a combination of the two being most effective. Thus, successful ventilation occurs first with good barn design. Barns must be spaced sufficiently far apart so as not to impair air movement because failure to do so will not only reduce air speed, but air will also become more humidified as it passes through a barn, thus becoming less effective in drying subsequent barns. Bewley et al. (2012) provide guidelines for proper sidewall openings and ridge vents to ensure natural ventilation, in addition to a discussion on fan types and selection.

Stirring of the pack is the management strategy which most differs from those applied to the conventional bedded pack. Stirring typically occurs twice each day, with milking time providing a convenient time during which cows are off the pack. It serves to increase pore space and break aggregates, and is critical because aerobic microbes are continuously consuming available oxygen. Further, the action serves to more thoroughly mix added materials into the pack, and relieves compaction caused by everyday cow

traffic. In addition to maintaining an overall aerobic environment for active composting, this results in a dry, fluffy surface on which cows can lay.

Bedding addition impacts the pack in two ways. The first is by altering WFPS; differing physical properties among materials result in variation in the degree to which WFPS is impacted by bedding. The second is through microbial nutrient availability. The CBP should maintain a C/N ratio of approximately 25:1 to 30:1 (Bewley et al., 2012). Bedding is added to increase C/N ratio, but even materials with a similar C/N ratio may metabolize differently; Janni et al. (2007) suggest that the higher lignin in wood products, their large surface area to volume ratio, and minimal packing between stirrings may be reasons for the observed success of fine dry wood products. Shane et al. (2010) observed similar pack performance across various materials to include sawdust, flax straw, wood chips, oat hulls, soybean straw, and “strawdust.” Pack temperatures indicated all materials supported microbial activity and produced heat, even with similar chemical characteristics to sawdust packs. However, they noted that most producers mixed in sawdust even when using alternative materials; it may be that sawdust provides the lowest volume of material for the highest C/N ratio, a factor of particular concern for farms with limited space for storing bedding materials.

Success has also been seen in compost bedded pack barns that don't utilize additional bedding material. Three farms with CBP barns in Israel were observed, and the NH<sub>3</sub> emissions measured. The study found NH<sub>3</sub> emissions to be ten times lower from the compost pack compared to the scraped feed alley. Researchers hypothesized that this difference is possibly due to the high C/N ratio and nitrogen-binding bacteria within the compost (Klaas et al., 2010). This is an important result because diet effects are

eliminated because both manure types are from the same cows; it also demonstrates that what the barn is bedded with may not matter as much as maintaining proper moisture conditions and C/N ratio in support of an optimally composting microbial population.

Perhaps the most obvious producer control is the cows themselves, because they contribute nearly all moisture and most nutrients to the system. Greater space per cow allows the pack to go longer between bedding additions because it takes longer for the material to reach its water holding capacity. Holsteins should be provided 9.3 m<sup>2</sup> resting space per cow and Jerseys 7.9 m<sup>2</sup> resting space per cow, with increases of space also needed for higher-producing cows due to their larger moisture production (Bewley et al., 2012). Stocking density most directly impacts moisture content, and cows decrease WFPS by compacting material as they move about and lay on the pack. They also contribute microbial biomass directly, in addition to supplying nearly all N for microbial transformations. Eckelkamp et al. (2016) noted that streptococci bacteria decreased with higher compost internal temperatures and were negatively correlated with stocking density as well as C/N ratio, suggesting that managing the pack for decreased MC and increased temperature may limit streptococci growth.

### 1.2.4. Influence of CBP on cows

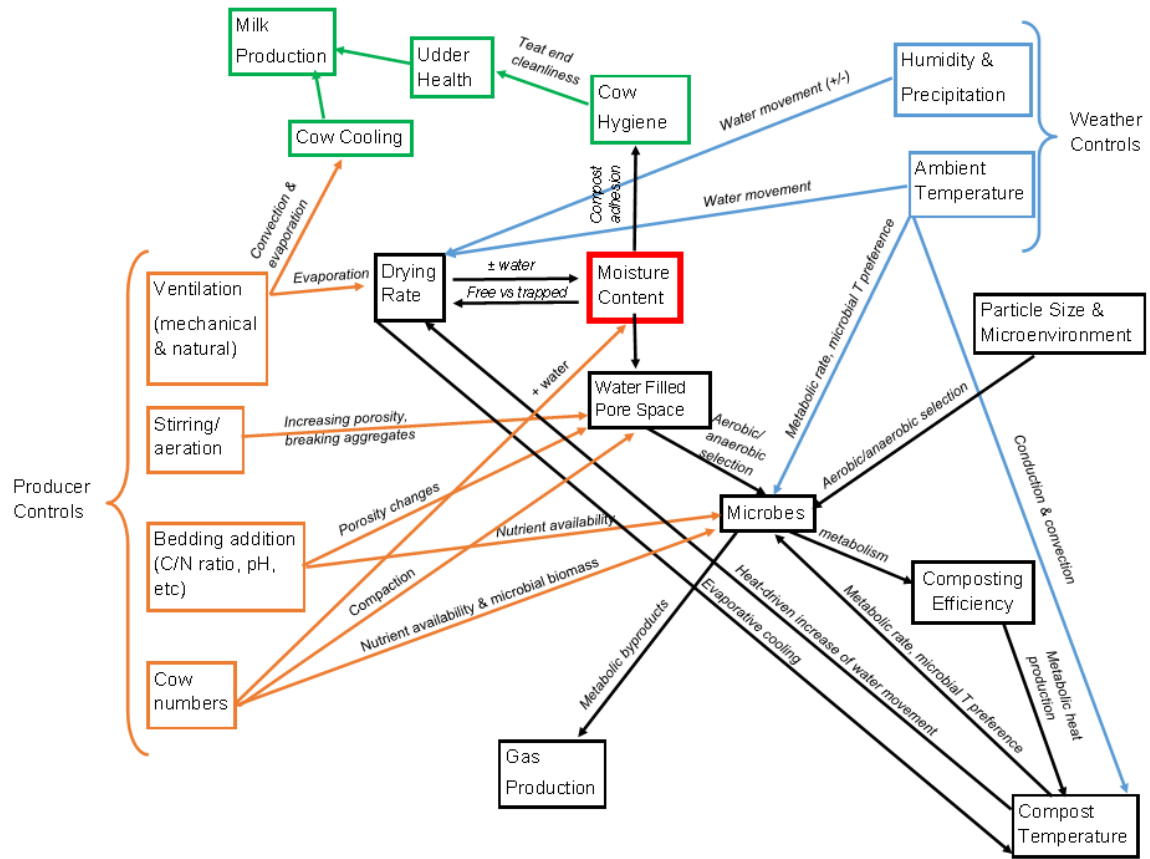


Figure 1-4. Diagram of the relationships between processes within the compost bedded pack barn environment and their impact on cow health and productivity.

The goal in managing any dairy facility (including the CBP) is optimizing the cow environment for maximal profitability. The importance of ventilation on cow cooling has already been mentioned; however, the pack itself has an influence on cows, largely dependent on pack MC (Figure 1-4). A higher MC increases the ease with which material sticks to cows; ultimately managing for reduced MC improves cow hygiene (Black, 2013). Eckelkamp et al. (2016) found herd hygiene in a CBP to remain below a score of 3 (solid plaques of dirt with hair visible) with both MC and barn temperature as predictors. A concern of early university researchers and farmers alike is the expectation of mastitis-causing pathogens to be in greater concentration in an environment as

seemingly dirty as the CBP barn. A survey of farms conducted by Black et al. (2014) showed that MC and space per cow impact the concentration of mastitis-causing pathogens. Higher MC enabled more material to stick to the cows; managing the pack for a dry resting surface can help prevent increases in SCC and mastitis.

Despite the high concentrations of bacteria within the pack, herds switching from freestall systems in Kentucky have had multiple improvements in production, likely due to the increased cow comfort provided by the CBP. “Cow comfort” is a term researchers occasionally shy away from because it cannot be measured directly; however, cow comfort improvements can manifest themselves in other areas, which can be observed. Lameness is an especially critical issue within the dairy industry due to both economic and public perception challenges. Huxley (2013) in a review of lameness studies noted an overall decrease in time eating with increasing lameness; while interactions are complex, generally a lame cow experiences production losses over a lactation of 270 to 574 kg. Improved cow comfort was the greatest benefit cited by producers switching to a CBP (Black et al., 2013). Decreased SCC even with a higher concentration of pathogenic bacteria in the bedding suggests an immunological benefit of improved cow comfort, and contrasts previous expectations which were based on the conventional bedded pack.

#### *1.2.5. Summary*

Moisture content is the central variable of concern in managing the CBP. However, it is important to understand that the relationships between CBP variables create a “web” of relationships rather than a simple linear process; individual components cannot be separated. Producers must manage multiple variables to optimize the cow



environment for greater productivity. While daily bedding costs are higher compared to traditional housing methods, initial barn investment is lower; further, the increase in cow comfort resulting in higher milk production and lower SCC may provide an economic benefit. The unique management style should result in a different GHG emissions profile than conventional housing and manure storage systems.

### **1.3. General dairy emissions**

#### *1.3.1. Introduction*

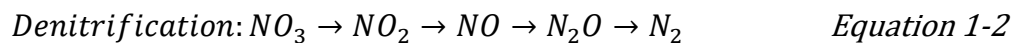
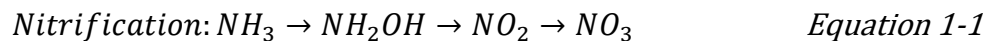
Ruminants represent an important component of global food security as they can process human-inedible food, a critical advantage to consider when comparing efficiency among species. Similarly, future regulatory decisions must balance food security with climate change, often competing challenges (Gill et al., 2010). To that end, of the 1.23 kg CO<sub>2</sub>e per kg fat corrected milk (FCM) in fluid milk consumption, 72% is associated with on-farm factors (Thoma et al., 2013). The US dairy industry is working to improve environmental performance of the supply chain in a way that is economically sustainable.

The challenge in directly limiting emissions is that costs and efforts to do so are, to a degree, diverted from actual production. Costs of dairy greenhouse gas regulation are highly variable between counties; largely, it seems that small farms would be less able to adapt to regulatory changes because they are less likely to be capable of investing in abatement technologies, such as methane digesters (Njuki & Bravo-Ureta, 2015). Thus, the general consensus among researchers is that priority in dairy emissions reduction should go to improving efficiency. Gill et al. (2010) noted that improving knowledge related to increasing efficiency within livestock production systems would

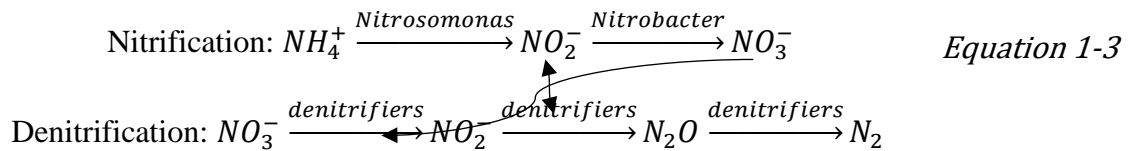
enable choices that would lead to decreased emissions. Likewise, Knapp et al. (2014) pointed out the importance of evaluating emissions in the framework of production because farmers won't implement mitigation strategies that cut production, and because increasing world population means agriculture as a whole must focus on improving efficiency. Liang et al. (2017) observed that GHG emissions are negatively correlated with milk production because high production dilutes emission from maintenance.

### 1.3.2. Overview of GHG processes

In general, CO<sub>2</sub> emissions from livestock and plant respiration are not considered significantly problematic in the context of climate change because they are part of a continuous biological process (Knapp et al., 2014). While the main source of CO<sub>2</sub> emission is fossil fuel, agricultural practices contribute 40% and 90% of global CH<sub>4</sub> and N<sub>2</sub>O. Nitrification (Equation 1-1) is the process of ammonium oxidation to nitrite and nitrate, with N<sub>2</sub>O as a resultant byproduct especially of anaerobic denitrification (Equation 1-2). *Nitrosomonas* under low oxygen conditions in particular reduce nitrogen dioxide and NO to produce N<sub>2</sub>O (McDowell, 2008). Fungi are known to be heavily involved within compost systems (Paul, 2014); the heterotrophic nitrification and denitrification processes follow a similar pattern as those used by autotrophs. The processes are understood generally as follows:



While denitrification is considered an anaerobic process due to facultative anaerobes performing most efficiently in an aerobic environment, the heterogeneous environment of a compost system leads to the formation of anaerobic microsites and often results in coupled aerobic and anaerobic activities such as coupled nitrification denitrification (CND, Equation 1-3). CND occurs primarily in aggregated, agricultural soils where large aggregates are present. Although such aggregates have negligible contributions to nitrification, their presence facilitates anaerobic processes even within aerobic profiles; the overall CND process is shown below as proposed by Kremen et al. (2005).



### 1.3.3. Potential control points for dairy GHGs

Optimization of cow diets has also been a focus in emissions control. Grazing dairies, though often perceived by consumers to be more environmentally friendly, have a significantly lower feed nitrogen use efficiency (FNUE), likely due to the lower diet control (Gourley et al., 2012). However, Cabezas-Garcia et al. (2017) in evaluating methane production noted that genetic variation among cows may play an even bigger role than nutrition alone.

In addition to optimizing the cow environment, manure storage is an obvious emissions control point. Methane digesters have become another increasingly examined

option. Temperature has an effect on the gas emission profile of anaerobic digesters, with a higher temperature resulting in higher methane emissions. Methane digesters also had high ammonium recovery. However, they are currently expensive to set up and relatively impractical for smaller farms (Umetsu et al., 2005).

Amon et al. (2001) used FTIR spectroscopy to measure emissions of ammonia, N<sub>2</sub>O, and CH<sub>4</sub> from a slurry, manure directly on straw, and compost. Fresh air was pulled into a small chamber, and spectroscopic measurements taken at the inlet and outlet. Net substrate emissions resulted from the difference in concentrations between the two measurement points. No significant difference was observed in NH<sub>3</sub>, N<sub>2</sub>O or CH<sub>4</sub> between the slurry and manure on straw. During storage, compost NH<sub>3</sub> emissions were higher than the slurry in both winter and summer; however, the compost was turned only seven times in the 80 day storage period, and it was noted by researchers that more straw could also increase C/N ratio. Compost NH<sub>3</sub> emissions were undetectable after spreading, compared to stacked losses of 2.8 kg NH<sub>3</sub> ha<sup>-1</sup> in summer, and 5.74 kg NH<sub>3</sub> ha<sup>-1</sup> in winter. Further, 81% of total NH<sub>3</sub> emissions for stacked manure occurred after spreading. Anaerobically stacked manure emitted about 4.5 times more greenhouse gases (N<sub>2</sub>O and CH<sub>4</sub>) than aerobically composted manure in the summer (61.49 kg CO<sub>2</sub> equivalents vs 13.83 kg CO<sub>2</sub> equivalents). This difference was not seen in the winter because the compost was not sufficiently aerated, allowing the system to also become anaerobic. The recommendations at the conclusion of the study were to widen the C/N ratio, aerate frequently, store everything on concrete, and manage storage area borders to minimize runoff and seepage.

#### *1.3.4. Summary*

In a developed country such as the US, where nutrition is mostly optimized, the biggest opportunities for emissions reduction occur in improving genetics and allowing cows to reach genetic potential by working on other management factors as is already done to improve cow efficiency (Knapp et al., 2014). The CBP fits into this picture by providing improved cow comfort. Additionally, manure management is a key factor determining emissions and runoff of nutrients from dairy operations. The study by Amon supported that composting should reduce overall emissions. However, the CBP barn may have even greater potential in emissions reduction. The CBP barn is an intensively managed dairy housing system in which manure is not scraped away to a separate storage facility as seen in most housing types; rather, it is composted in place. A liquid storage facility, in most situations, is still necessary to handle waste from the feed alley, but the vast majority of the manure and urine from cows ends up on the pack. Compost bedded pack barns differ from the traditional bedded pack in how they are managed. The traditional bedded pack barn has a pack of material on which the cows rest, and more is added as-needed to keep cows mostly clean and dry, much like the CBP. However, the simple bedded pack is not stirred, resulting in a largely anaerobic system. This anaerobic system results in less microbiological diversity and less efficient material breakdown. Further, breakdown of materials in the absence of oxygen results in higher levels of undesirable emissions, such as  $\text{NH}_3$ . Denitrification in an anaerobic environment is also more likely to produce  $\text{N}_2\text{O}$ . Ultimately, the primarily aerobic processing of materials should shift non-enteric emissions to a higher percentage of  $\text{CO}_2$ .

#### **1.4. Chamber design to measure GHG emission**

Measurement chambers have been a widely used method of determining gas emissions from soil and some livestock facilities. The two primary chamber classes are open and closed; both types have been used with fans (dynamic) and without (static). In the open dynamic method, air is forced through the chamber at a known rate and concentrations of gases of interest are measured at each location. In the closed static system, a chamber with no other openings is placed on top of the soil, and the slope of the concentration curve is used to determine emission rate. Variations have also been attempted such as open with only natural air movement, and closed with fans to force mixing within the chamber. However, multiple design challenges are associated with each method.

##### *1.4.1. Background*

Because the goal of the chamber is to determine an emissions rate representative of the test area, it is obviously desirable to disrupt the natural emissions processes as little as possible. Thus, concerns such as pressure differences and diffusion gradients must be immediately addressed. Any chamber will disrupt either or both of these to some degree. Hutchinson and Mosier (1981) addressed a few of the differences in the open versus closed chamber debate, pointing out several reasons a closed chamber may be more effective. Because gases emitted to a closed cover are not continually diluted, they were able to detect smaller fluxes. Additionally, they established that an open cover must be operated at sub-ambient pressure to establish flow-through air circulation, which provides an opportunity for mass flow from soil outside the chamber. Although they admitted that

the decreasing diffusion gradient within a closed chamber may have an effect on N<sub>2</sub>O production and thus emission, inferring the emission rate at cover time from the accumulation curve could eliminate this effect.

Jensen et al. (1996) compared static and dynamic methods for measuring soil CO<sub>2</sub> as an index of soil respiration and found variation in the success of the two methods. Sodium hydroxide was used to absorb CO<sub>2</sub> in both cases. The static method showed fluxes 12% higher when the rate was under 100 mg CO<sub>2</sub>-C m<sup>-2</sup>h<sup>-1</sup>, yet up to five times lower when the flux was greater than 100 mg CO<sub>2</sub>-C m<sup>-2</sup>h<sup>-1</sup>. The static chamber had a cap which was removed at placement to minimize initial pressure disturbances, and the dynamic chamber had fans for mixing at low speed. They were able to correct diurnal temperature differences with Q<sub>10</sub>, but suggested lots of replications to account for other variability day-to-day. Additionally, they found that neither chamber performed better than the other on either the sandy loam or coarse sandy soils tested.

Another concern somewhat independent of chamber type or mixing is leakage from the chamber, above and below ground. As concentration increases within the chamber, a reverse gradient develops within the soil profile. Gases may diffuse laterally in the soil for movement across a more favorable pressure or diffusion gradient; this type of leakage is a function of chamber geometry, depth of gas production, soil air filled porosity, and the soil gas diffusion coefficient (Li & Group, 2000). A collar embedded within the soil under the chamber addresses this problem, but brings with it several other questions, such as insertion depth, timing of placement, and attachment to the primary chamber piece. Typically in soil science, it is suggested to place the collar well before the chamber (Timothy B Parkin & Venterea, 2010), but this is primarily to minimize the

effects from disturbing roots, which is not a concern in livestock systems. In the case of the collar being a separate piece from the chamber, a groove is often implemented between the two and filled with water after placement. Depth of placement is highly variable between studies, but ranges from 2.5 cm (Hutchinson & Livingston, 2001) to at least 8 cm (Parkin & Venterea, 2010).

Several factors may determine whether open or closed chambers are better for each situation. Closed chambers may permit greater control of airflow over the soil surface, but this may not be representative of the actual environment. Additionally, a pressure buildup within the chamber with time will decrease any mass flow from the soil, and diffusion will decrease in response to a decreased concentration gradient between the soil and the chamber air. Vents also assist in maintaining both temperature and moisture similar to field conditions (Xu et al., 2006). Davidson et al. (2002) suggested that all chambers should have vents to equalize pressure. However, care must be taken in designing such vents. Conen and Smith (1998) noted higher N<sub>2</sub>O emissions on average from vented chambers, and pressures consistently below ambient which could only be caused by a continuous removal of air, caused by the Venturi effect.

Xu et al. (2006) similarly noted that because past studies attempting to relate pressure differences to mass flow were inconsistent, it is necessary to instead minimize the Venturi effect. Bernoulli's equation was used to develop a novel vent design that slows wind using a tapered "T" over a vent at the top of the chamber. First, they examined the original design without the T-piece on both an impermeable and soil base. They found that on the soil base, no pressure difference was observed from ambient. However, on the impermeable base, a pressure difference developed. This showed that



mass flow was occurring from the soil before a pressure difference could exist, resulting in apparently higher emissions rates. Bain et al. (2005) showed similar results and correlated a 1 Pa drop in pressure for each  $1 \text{ m s}^{-1}$  increase in air velocity across the vent opening. Xu et al. (2006) also noted that the impact of positive pressure as would develop in a closed chamber may be less than that of the negative pressure as a result of a poorly designed vent, and that the complex relationship between pressure difference and gas flux measurement makes post-experiment corrections limited in value. The T-design for their vent used a ratio in diameters similar to the ratio of the wind velocity near ground level and wind velocity at the entrance of their T-piece. The wind velocity profile was initially estimated based on the landscape, but measurements confirmed their estimate in both grassy and low shrub conditions, with a ratio of 1:5 working well.

The use of fans in chambers is also widely debated. Some have suggested that fans introduce pressure perturbations that result in different fluxes than would be observed naturally (Parkin & Venterea, 2010; Pumpanen et al., 2004). However, Christiansen et al. (2011) used a reference gas in a laboratory setup to compare effects of mixing and found that fan-mixed chambers resulted in significantly lower normalized root mean square error than chambers with no mixing. Moreover, measured fluxes from the mixed chambers were significantly closer to the flux expected from the reference gas. Designing chambers with a small volume to headspace height ratio can also minimize the need for mixing and produce increased chamber sensitivity (Parkin & Venterea, 2010).

A few studies have applied the chamber measurement method to livestock systems. Brewer and Costello (1999) used an enclosed air chamber with an infrared gas analyzer to monitor broiler house ammonia volatilization. The measurement was precise

enough to identify trends related to position in the broiler house, and air speed within the chamber was kept within 12% of the typical air movement. The chamber utilized a 38 mm sheet metal collar, allowing it to penetrate the litter. Amon et al. (2001) used a chamber and FTIR to analyze  $\text{NH}_3$ ,  $\text{N}_2\text{O}$ , and  $\text{CH}_4$  emissions from dairy compost and anaerobically stacked manure by completely enclosing manure heaps. Both studies used a large flow-through chamber, controlling air flow rate and continuously monitoring gas concentration at inlet and outlet. One concern is whether forced air movement is representative of air movement within the normal environment; even if air flow rate is similar, air of low concentration of the gases of interest relative to ambient in the housing may result in a larger concentration gradient and thus greater diffusion.

#### *1.4.2. Application to the compost bedded pack barn*

In attempting to apply such studies to the compost bedded pack barn, it is clear no perfect method has already been developed. Some design considerations are already obvious. Unlike most previous studies, root development is not a concern, so a collar for the base of the chamber can only be beneficial, and could be placed at the same time as the chamber. Parkin and Venterea (2010) provides a thorough reference on chamber-based gas flux measurements, recommending deployment no longer than 60 minutes to minimize effects on MC and thus biological activity; measurements should occur over a range of times to capture the temporal variability, and an adequate number of chambers should be deployed to sufficiently represent the area. Ideally, the chamber should be deployed into the barn instead of placing compost within it so the temperature gradient is

maintained. The two main considerations remaining, then, are whether to utilize fans and whether to utilize the open or closed design.

The simplest and least expensive design would be a closed chamber with a low profile and gas measurement at a single point at the center of the chamber. However, compost has a unique potential for high humidity conditions due to its high MC and high temperature. A buildup of moisture in the chamber headspace may not only result in measurement errors, but could alter the diffusion process so that the gas buildup curve is not representative. A large chamber with straight flow-through air and sensors at both ends should keep moisture and temperature at appropriate levels, but the flow rate and content of that air would have to be similar to air at that height throughout the barn because clean air would result in a higher diffusion gradient; moreover, the concentration difference is likely to be excessively small in relation to the error of the sensors being used. A third option is utilizing the T-piece design presented by Xu et al. (2006), monitoring air speed at inlet and outlet, and monitoring gas concentrations at inlet, outlet, and chamber headspace; while this method may be most representative because the airflow should be most similar to conditions without the chamber, it is obviously the most cost-prohibitive. Several experiments may address the degree to which measurements are affected by these design options.

If the closed chamber design can work in the humid compost environment, this may be the best option as it requires the fewest components and more chambers could be deployed. Compost could be placed in a container in the lab and a water bath used to keep an appropriate temperature. A closed chamber containing sensors for gas concentration, relative humidity and temperature would demonstrate how functional the

system is as humidity increases, or even whether the humidity increase is substantial enough to be of concern after just an hour of measurement. Alternatively, a known concentration of a gas of interest could be supplied while the chamber is kept at a high humidity.

The T-piece design may only require two gas sensors, depending on air movement within the chamber. Inlet measurements should be conducted, but if there is sufficient mixing occurring so that there is no gas buildup within the headspace, only inlet and outlet measurements may need to occur. Similarly, if gas that diffuses into headspace does not leave the chamber over the measurement period and outlet concentration is similar to inlet concentration, only the inlet and headspace need sensors. Three sensors would be required in the case of concentration varying at all three locations over the measurement period.

## **1.5. Objectives**

The overarching objective of this study is to design and test a low-cost gas emissions chamber for use in CBP barn environments. The individual objectives are as follows:

- 1) Fabricate a prototype emissions measurement chamber using off-the-shelf components.
- 2) Calibrate low-cost CH<sub>4</sub>, CO<sub>2</sub>, and NH<sub>3</sub> gas sensors individually and when used in an emissions measurement chamber.
- 3) Deploy the emissions chamber in a CBP barn to gather preliminary data on important gas emissions rates.

## **CHAPTER 2: Prototype Emissions Measurement Chamber**

### **2.1. Introduction**

The composting environment elicits the need for a unique set of chamber requirements as outlined in Chapter 1. The static chamber layout was chosen, with a small fan included to disrupt the boundary layer, and sensors for humidity, temperature, NH<sub>3</sub>, CO<sub>2</sub>, and CH<sub>4</sub>.

Overall, the measuring chamber design is based on the use of sensors able to measure at a high frequency. This contrasts typical systems that require manual withdrawal of air several times per hour, and with a substantially lower cost than a photoacoustic measurement system. The comparatively low precision of individual sensors is offset by the increase in measurement frequency without an increase in labor or system disturbances. Moreover, the chamber system is less likely to miss important changes, as often occurs when only several points per hour are used to infer emissions (Parkin et al., 2012). The small chamber size results in less averaging of microsites than large systems; thus, many chambers should be used to adequately capture the spatial variation of the system, but “many” is economically feasible due to the lower cost per chamber and allows further geostatistical analysis (Woodbury et al., 2006).

### **2.2. Materials and Methods**

A stainless steel mixing bowl was used as the chamber shell, with a footprint of 0.05 m<sup>2</sup> and a headspace volume of 5.4 L (excluding space taken up by components within the chamber). A 120 mm diameter pulse width modulation (PWM) fan was included with variable speed; an air movement rate over the compost of 1 m s<sup>-1</sup> has been demonstrated to adequately disrupt the boundary layer of physically similar surfaces

(Ferguson et al., 1998; Gates et al., 1997). Sensors for temperature and humidity were suspended centrally in the chamber headspace and connected to a Measurement Computing USB-2408 DAQ board (Measurement Computing Corporation, Norton, MA).

Infrared sensors were purchased to measure CO<sub>2</sub> and CH<sub>4</sub>, and an electrochemical sensor was purchased for NH<sub>3</sub>. Each of the two types was purchased with its own evaluation board and software to process the voltage and current outputs as needed.

### *2.2.1. Infrared sensor*

Infrared measurement relies on the principle that molecules are excited by light, resulting in particular absorption patterns due to vibrational activity. Molecules that are asymmetrical or have vibrational modes resulting in net dipoles can be measured by IR sensors. One challenge with gas detection using IR is working within “water windows,” especially at higher humidity. Peaks due to water have the potential to overlap those of the gases that need to be detected; the most useful zones are those that include gases of interest but exclude water. A range of 3 to 5 microns allows detection of CO<sub>2</sub> around 4.2 microns and hydrocarbons from 3.5 to 5 microns.

The IR sensor initially chosen was an IR15TTR. This device detects both CO<sub>2</sub> and CH<sub>4</sub> at a range of 0-100% and includes an internal thermistor. It operates a few degrees above ambient temperature due to heat generated by the IR lamp; this heat also serves to offset some water condensation. The IR15TTR was eventually replaced with similar sensors operating over a smaller concentration range once it was determined concentrations in the field would be too small to detect using a 0-100% sensor. CO<sub>2</sub> was measured with IR15TT-M, while IR22EJ was purchased to measure CH<sub>4</sub>.

An IR evaluation board (IR-EK2, SGX Sensortech, High Wycombe, UK) was purchased along with the sensor. The board itself is powered by a 9 V DC supply and connects to a computer via USB. Accompanying software was installed on the computer. The first tab in the program (Figure 2-1. First tab of SGX software. Figure 2-1) has a monitoring area to visualize various outputs from the board, adjustable by a drop-down menu. The lamp, reference, and channel voltages were set by adjusting the potentiometers on the board until the various voltages approximately reached recommended values. This is a critical initial step. The third tab (Figure 2-2) is for sensor calibration; a coefficient editor is available when in device setup mode which by default pulls from the installation CD the parameters recommended by the company for converting voltages to concentrations, and the “Set Span” and “Set Zero” buttons enable a two-point linear calibration of the sensor.

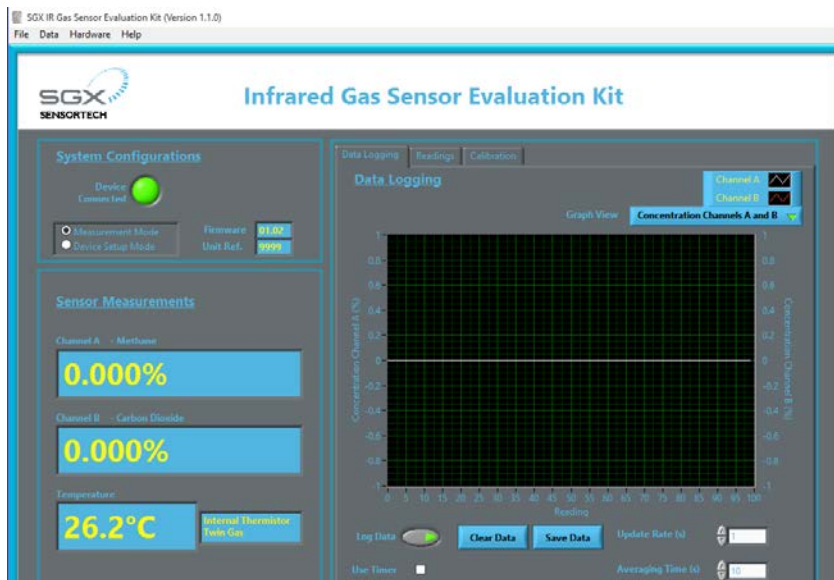
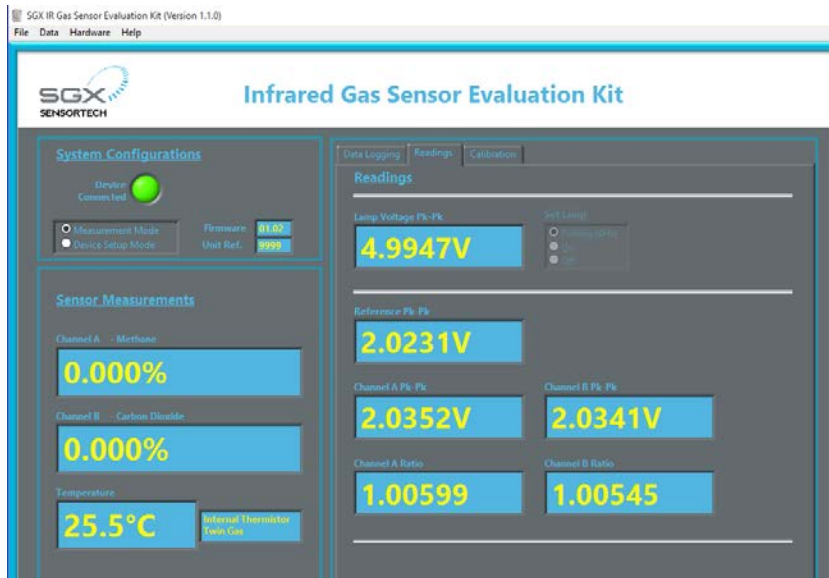


Figure 2-1. First tab of SGX software.





*Figure 2-2. Voltage adjustment tab of SGX software.*

### 2.2.2. Electrochemical sensor

Electrochemical sensors function by creating a chemical reaction between the gas and oxygen contained in the sensor, resulting in a current proportional to the gas concentration. The electrochemical sensor was a 0-100 ppm  $\text{NH}_3$  sensor, SGX-7NH3 (SGX Sensortech, High Wycombe, UK). A thermistor is also present to measure ambient temperature. The evaluation board purchased for this sensor type (ECVQ-EK3, SGX Sensortech, High Wycombe, UK) similarly uses a 9 V<sub>DC</sub> and a USB connection. Separate software was installed for electrochemical evaluation. The calibration process is identical to the IR sensor using the appropriate gas.

Approximate values for sensors were already determined by SGX Sensortech and were provided for easy download to the program; calibration allows these to be adjusted for the specific sensor in use. The original software provided an excellent interface for the calibration process; however, it was primarily intended for calibration and had

limitations when it came to long-term data collection. Specifically, although a data saving function was available, it was not logged moving forward, and previous data was not saved unless prompted by a user. Because data was only saved to memory as it was collected and not written to a file, this presented the risk of all data being lost if the process was interrupted.

### *2.2.3. Programming*

A program was developed in Microsoft Visual Studio (Microsoft Visual Studio 2015, Microsoft Corporation, Redmond, WA) to simultaneously record measurements from the gas, temperature, and humidity sensors (Figure 2-3). The program read inputs from three sources via USB: the DAQ board, the IR evaluation board, and the electrochemical evaluation board. A timer was implemented to trigger a measurement from all sensors every second. Voltages corresponding to temperature and humidity were read from the DAQ board output and converted to temperature (Celsius) and relative humidity (percent) within the program.

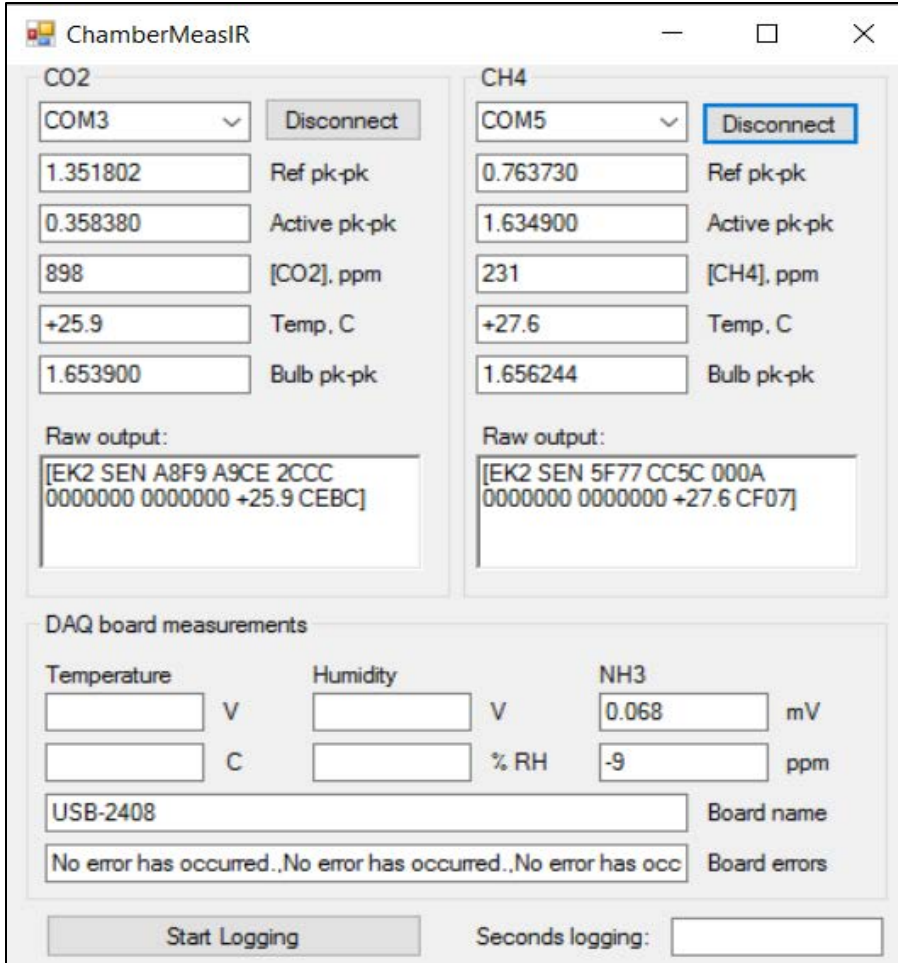


Figure 2-3. Program developed for data collection.

The IR reading was a string of several components, with brief user messages as text and numerical values represented in hexadecimal format. The SGX Sensortech evaluation kit user guide was referenced to determine how to process different components of the incoming string. Numerical readings included reference and active channel voltages, IR bulb voltage, temperature at the IR sensor, and concentrations as determined by the microprocessor on the evaluation board. Voltages were calculated by:

$$V_{IR} = D_{in} * \frac{2.048}{65535} \quad \text{Equation 2-1}$$

where  $V_{IR}$  is any of the infrared board voltage outputs and  $D_{in}$  is the digital reading.

The electrochemical board reading was similar to but slightly simpler than the IR reading because it was a single-gas sensor and because only the current was needed to calculate concentration rather than multiple voltages. The hexadecimal outputs could also be directly converted to current (nA) and concentration (ppm).

The program display allowed selection of COM ports with a “connect” button to initiate data reading. The raw output of each gas sensor was displayed, in addition to individual text boxes for each component after it had been converted to an appropriate, user-friendly format. A similar procedure occurred for the DAQ board readings where voltages were displayed in addition to temperature and humidity. A message box allowed easy observation of DAQ board errors.

Clicking the “Start Logging” button prompted the user to save a file to which time, IR reference peak-to-peak voltage (V), CH<sub>4</sub> active channel peak-to-peak voltage (V), CO<sub>2</sub> active channel peak-to-peak voltage (V), CH<sub>4</sub> concentration (ppm), CO<sub>2</sub> concentration (ppm), IR temperature (°C), IR bulb voltage (V), electrochemical bias voltage (mV), NH<sub>3</sub> concentration (ppm), electrochemical output current (nA), electrochemical calibration gas concentration (ppm), electrochemical calibration current (nA), electrochemical temperature (°C), electrochemical range (low = 5 nA, high = 25 nA gain per ADC step), electrochemical selected range, intra-chamber temperature sensor voltage (V), intra-chamber temperature (°C), intra-chamber humidity sensor voltage (V), and intra-chamber humidity (%) were recorded each second.

### 2.3. Results and Discussion

The original software from SGX Sensortech allowed calibration information to be written back to the microprocessor on the evaluation board so that concentrations could be calculated prior to being read by a PC. It was initially decided to neglect this feature from the new program, instead calculating concentration within the PC software. The drawback to this method is that the sensors, if connected using another program, may no longer produce accurate concentrations; this should not be a problem for this application of the sensors, but a small supplementary program was also written to enable writing to the microprocessor on each board.

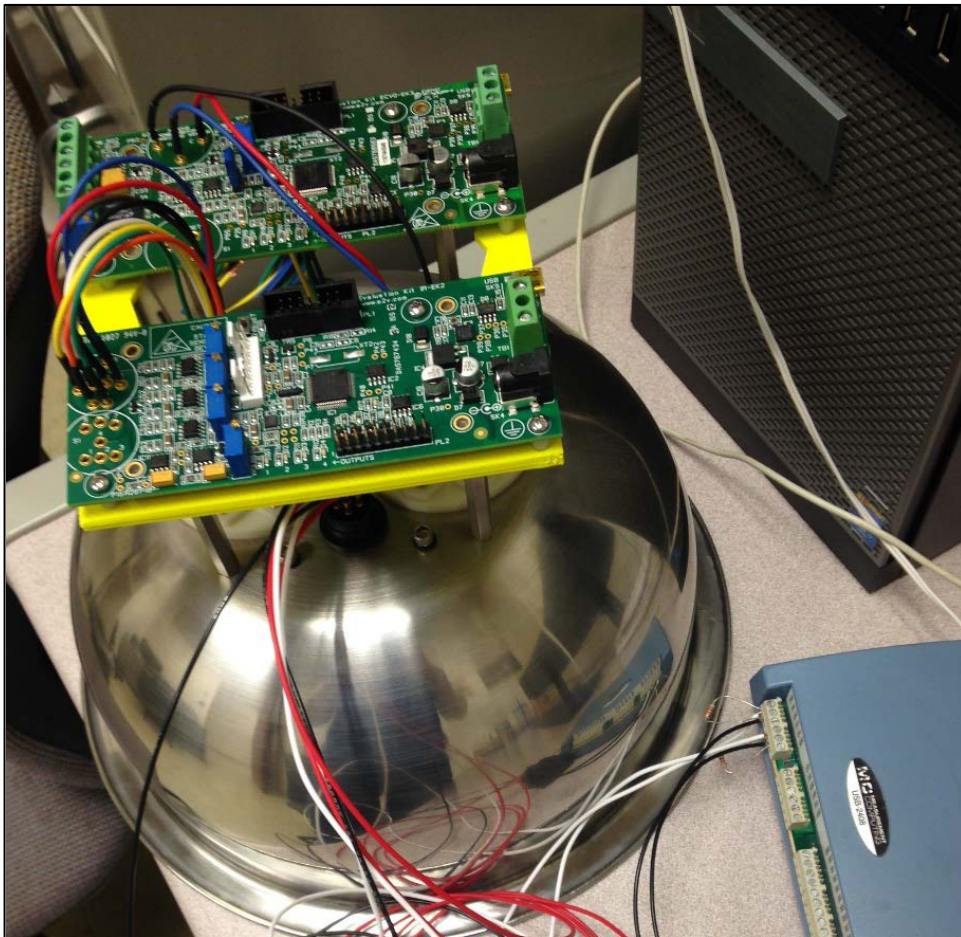


*Figure 2-4. Chamber prototype consisting of a mixing bowl, with sensors inserted in the top.*

## **2.4. Conclusions**

A chamber prototype (Figure 2-4) was developed that is less expensive than photoacoustic chambers and has a higher rate of data collection than gas chromatography methods. The next step is performing a two-point calibration with the system for each of the gases and with consideration to slightly different temperature and humidity possibilities.

## CHAPTER 3: Emissions Measurement Chamber Calibration

### 3.1. Introduction

SGX Sensortech provides estimations for calibration coefficients for their sensors based on values obtained in their lab. However, in the composting environment, temperature and humidity are expected to play an important role, and the fluxes measured are expected to be very small. Calibration helps to maximize sensor accuracy in the field.

### 3.2. Materials and Methods

#### 3.2.1. Calibration gases

Certified calibration gases were purchased for sensor calibration at zero and a “span” level equal to or below the sensor upper range, encompassing the values expected within the composting environment. Concentrations were chosen to be 100 ppm NH<sub>3</sub>, 100 ppm CH<sub>4</sub>, and 1500 ppm CO<sub>2</sub>. Concentrations were later determined via GC to be 8 to 578 ppm CH<sub>4</sub> and 531 to 6580 ppm CO<sub>2</sub>.

Gases were stored at room temperature. Flow rate was set to 1.5 L min<sup>-1</sup> with a Dwyer flowmeter operating at the lowest pressure possible as regulated with a Concoa valve.

#### 3.2.2. Individual sensor calibration

Gas sensors were first calibrated individually because calibrating the entire chamber simultaneously would be not only time-consuming, but susceptible to variation due to leaks. A gas line was run from the flowmeter to a small calibration chamber provided by SGX which fit tightly over the sensors (Figure 3-1); the low volume resulted in minimal purge time so that the sensor response could quickly be identified. The

system took from 1 to 5 minutes to stabilize, at which point the replication was considered complete. Three replications were conducted for each of the three sensors, with order determined using a random number generator. Gases were exhausted into a fume hood (Figure 3-2).

For the electrochemical sensor, the output current was used to determine the linear sensor response to gas concentration as outlined in SGX Sensortech Electrochemical Note 2. For the infrared sensor with both CH<sub>4</sub> and CO<sub>2</sub>, the voltage output of each channel was used to determine the exponential response as in SGX Sensortech IR Notes 2 and 5.

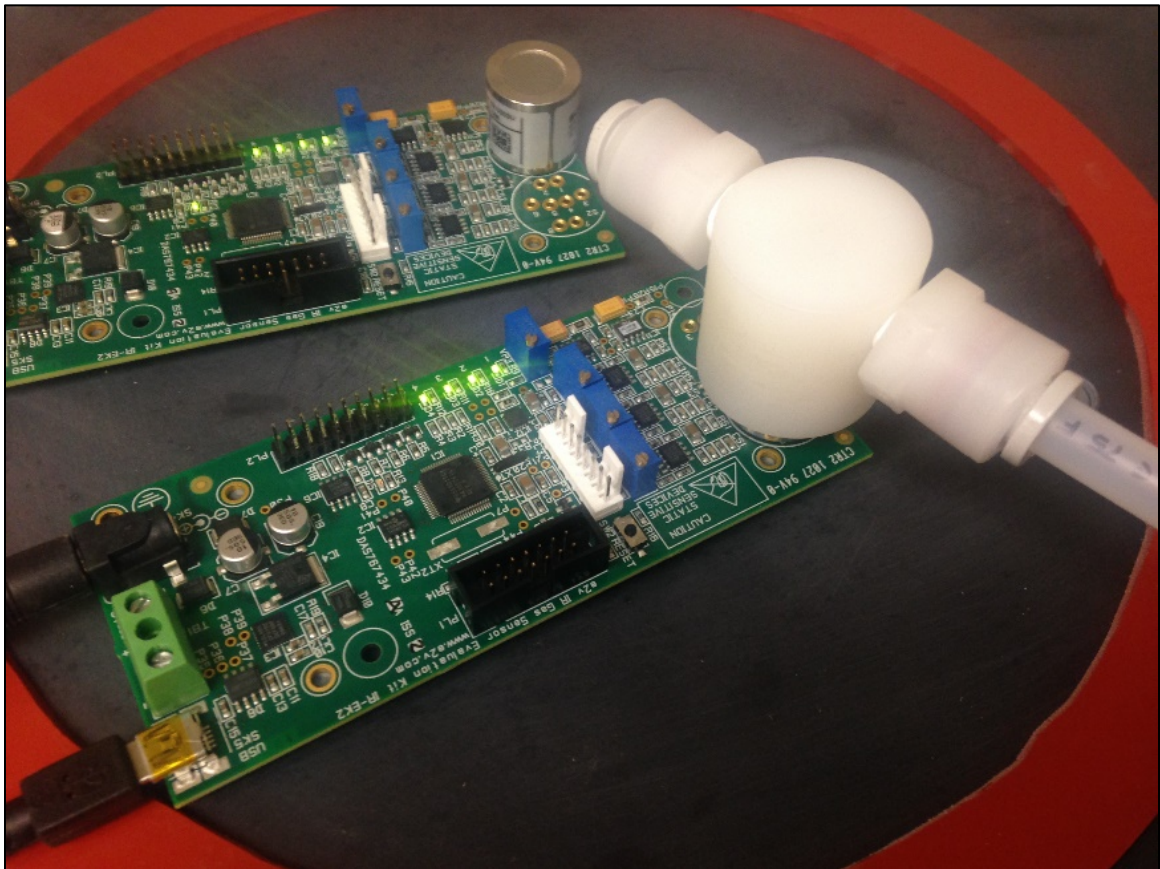


*Figure 3-1. Close-up of individual sensor calibration process.*





*Figure 3-2. Sensors were calibrated in a fume hood while the program ran on a tablet PC.*

### *3.2.3. Chamber calibration*

Once the sensors had been calibrated, the process was repeated with the chamber as a whole to determine the system response time to a step input. A mounting base was developed to seal the chamber and allow the flow of calibration gases through the chamber. Expected purge time was determined as a function of flow rate, chamber volume, and gas concentration change; having individual sensors already calibrated permitted easy comparison to the theoretical curve, with major variation suggesting a problem in chamber sealing.

### *3.2.4. Temperature and humidity*

The compost surface is expected to be within the operating ranges of the sensors for both temperature and humidity, especially during summer conditions (Eckelkamp, 2014); a MATLAB script (Appendix D) was developed to confirm time to saturation of chamber air, predicting whether condensation was likely. At typical summer conditions

of a low compost surface temperature and high ambient temperature, relative humidity in the chamber reached approximately 72%. However, both temperature and humidity may reach sufficiently extreme levels to influence concentration readings. Temperature and humidity sensors were calibrated in an environmental chamber at 25 C and 60% RH and at 13 C and 85% RH to permit a general idea of temperature and humidity during deployment. Field data at a later date confirmed that impacts were minimal, despite some condensation occurring late in post-stirring deployments.

### 3.3. Results and Discussion

A MATLAB script was written to determine the steady-state values for each replication, and the average steady-state values were used in the calibration equations. SGX Infrared Application Note 2 was referenced to approximate the concentrations as a function of the IR sensor outputs using the following equations:

$$Zero = \frac{V_{act,zero}}{V_{ref,zero}} \quad \text{Equation 3-1}$$

where  $V_{act,zero}$  is the active channel voltage in zero calibration gas, and  $V_{ref,zero}$  is the reference channel voltage in zero calibration gas;

$$Span = \frac{1 - \frac{V_{act,span}}{Zero * V_{ref,span}}}{1 - e^{-aC^n}} \quad \text{Equation 3-2}$$

where  $V_{act,span}$  is the active channel voltage in the span calibration gas,  $V_{ref,span}$  is the reference channel voltage in the span calibration gas,  $a$  is a calibration coefficient (estimated to be 1.01 by SGX),  $C$  is the span calibration gas in percent, and  $n$  is a calibration coefficient (estimated to be 0.675 by SGX);

$$NR = \frac{V_{act}}{Zero * V_{ref}} \quad \text{Equation 3-3}$$

where  $NR$  is termed the normalized ratio,  $V_{act}$  is the active channel voltage, and  $V_{ref}$  is the reference channel voltage;

$$NR_{comp} = NR * (1 + \alpha(T - T_{cal})) \quad \text{Equation 3-4}$$

where  $NR_{comp}$  is the compensated normalized ratio,  $\alpha$  is the temperature compensation coefficient (estimated to be 0.0005 by SGX),  $T$  is the temperature measured by the IR sensor, and  $T_{cal}$  is the temperature at which calibration was performed as measured by the IR sensor;

$$Span_{comp} = Span + (\beta * \frac{T - T_{cal}}{T_{cal}}) \quad \text{Equation 3-5}$$

where  $Span_{comp}$  is the temperature-compensated span value and  $\beta$  is the temperature compensation coefficient (estimated to be 0.3 by SGX); and

$$C_{ppm} = \left( -\frac{\ln\left(1 - \left(\frac{1 - NR_{comp}}{span_{comp}}\right)\right)}{a} \right) * \left(\frac{1}{n}\right) * 10000 \quad \text{Equation 3-6}$$

where  $C_{ppm}$  is the gas concentration in parts per million (v/v) and 10000 is the conversion factor from percent to ppm.

Upon initial application of the SGX equations, it was found that the concentration calculation consistently produced a result different from the certified calibration gas by some factor. The “a” and “n” coefficients were adjusted to minimize RMSE and both changed to a value of 1.

The electrochemical evaluation board produced currents which arbitrarily changed sign, suggesting the board was malfunctioning and the apparent signal output was simply noise. Assessing the sensor itself with a digital multimeter confirmed that the  $NH_3$  sensor individually was functional, although current outputs were not in the range

expected. A 100  $\Omega$  resistor was run between the output and ground electrodes to convert the current signal into a voltage signal and the DAQ board already in use for temperature and humidity sensors, producing a useful signal which allowed for calibration and potentially also data collection.

Steady-state for the ammonia sensor was found in a similar manner as the IR sensors. At near-ambient conditions, a linear response is expected; thus, the two-point calibration procedure was deemed adequate and calibration coefficients could be determined using  $y = mx + b$  in the form of

$$C_{pred} = \left( \frac{C_{span}}{V_{max} - V_{min}} \right) V - \frac{C_{span}V_{min}}{V_{max} - V_{min}} \quad \text{Equation 3-7}$$

where  $C_{pred}$  is the predicted ammonia concentration in ppm,  $C_{span}$  is the value of the maximum concentration gas in ppm,  $V_{max}$  is the voltage output at the maximum concentration,  $V_{min}$  is the voltage output at the minimum concentration (assumed to be zero in ambient conditions), and  $V$  is the voltage reading.

While the zero-gas readings were somewhat scattered due to noise in the DAQ board resulting in variable non-zero output, the slope was consistent. RMSE was calculated using the three calibration trials, allowing the development of the prediction intervals (Table 3-1).

$$95\% PI = \pm 2 * RMSE \quad \text{Equation 3-8}$$

Table 3-1. Prediction intervals for calibrated gas sensors.

Sensor	“Low” calibration gas concentration	“High” calibration gas concentration
CH <sub>4</sub>	0 ± 10 ppm	100 ± 15 ppm
CO <sub>2</sub>	0 ± 3 ppm	1500 ± 6 ppm
NH <sub>3</sub>	0 ± 3 ppm	100 ± 6 ppm

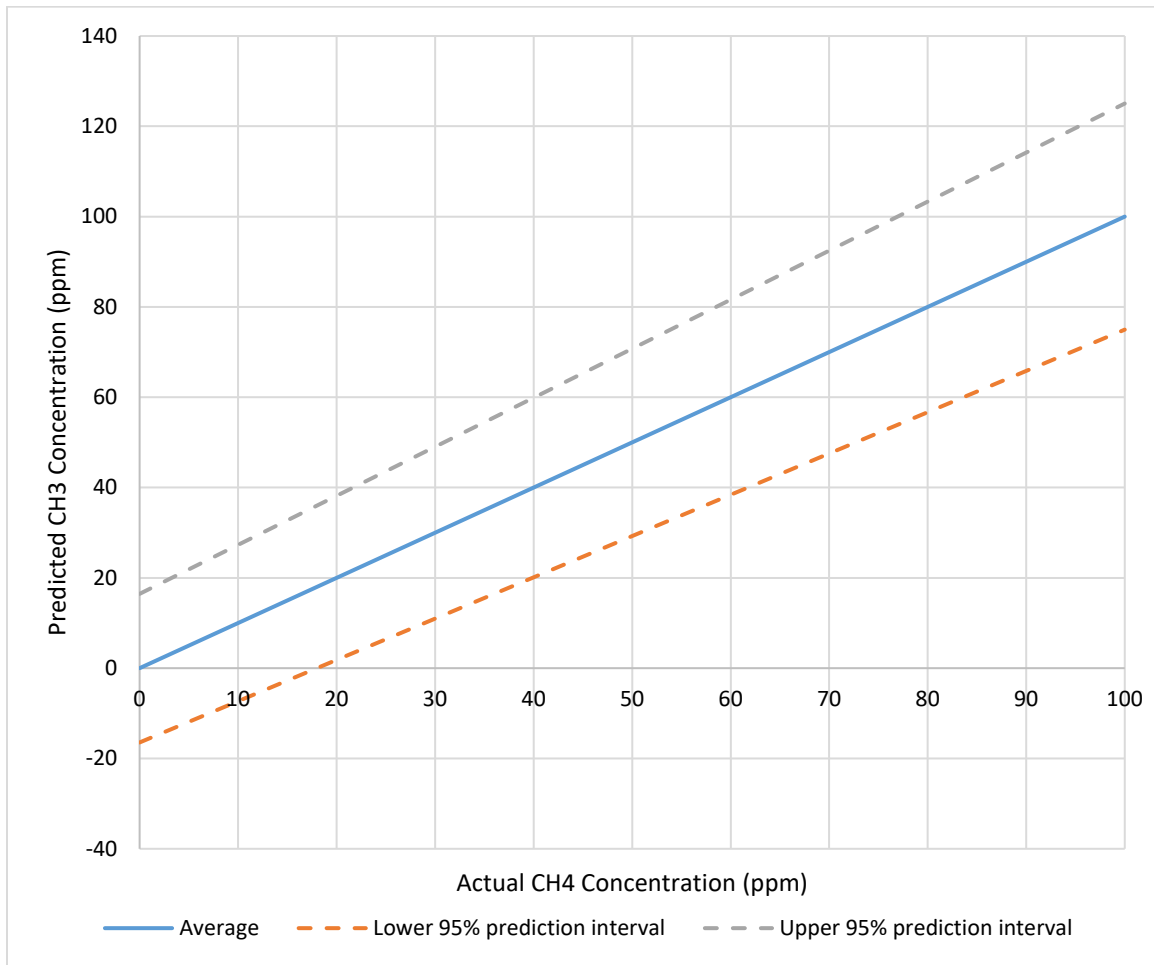
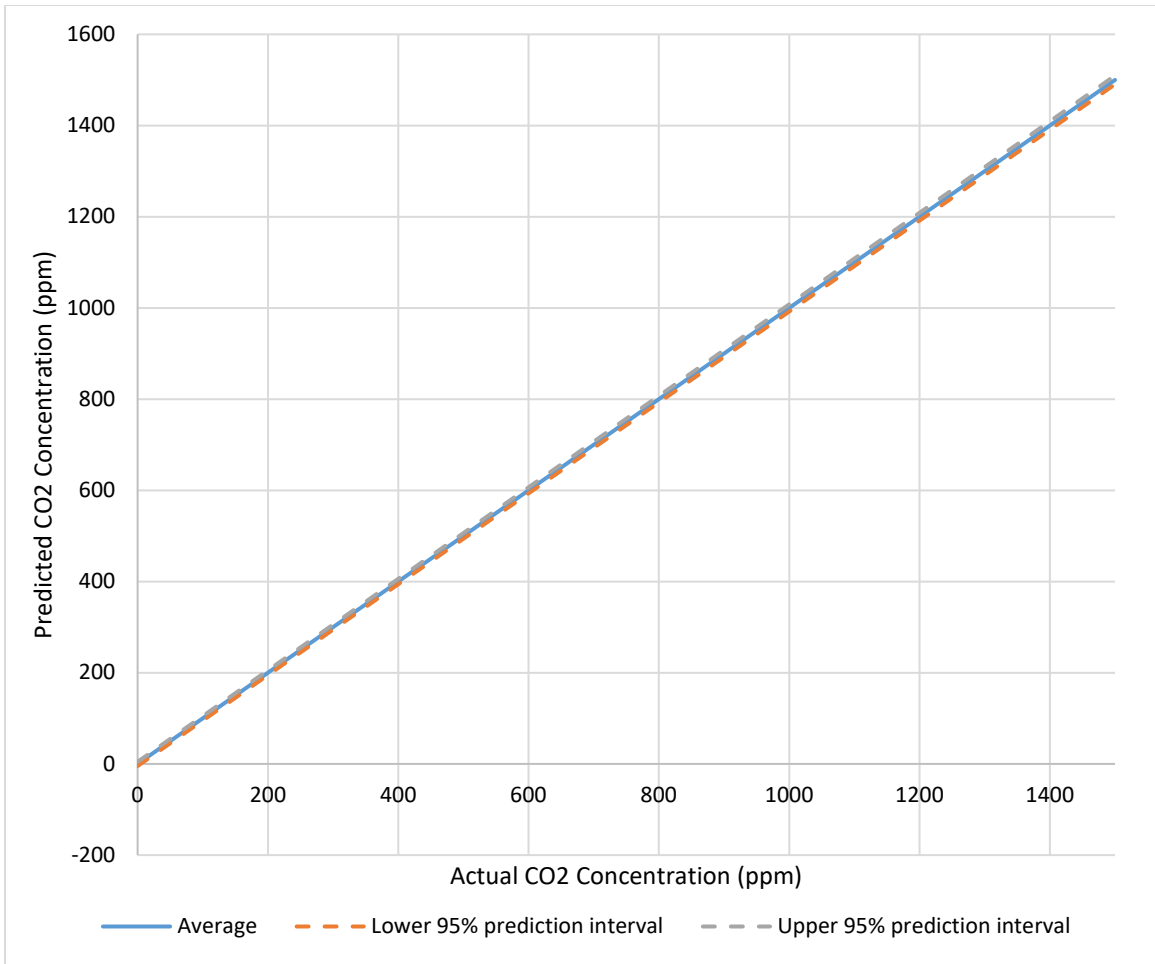
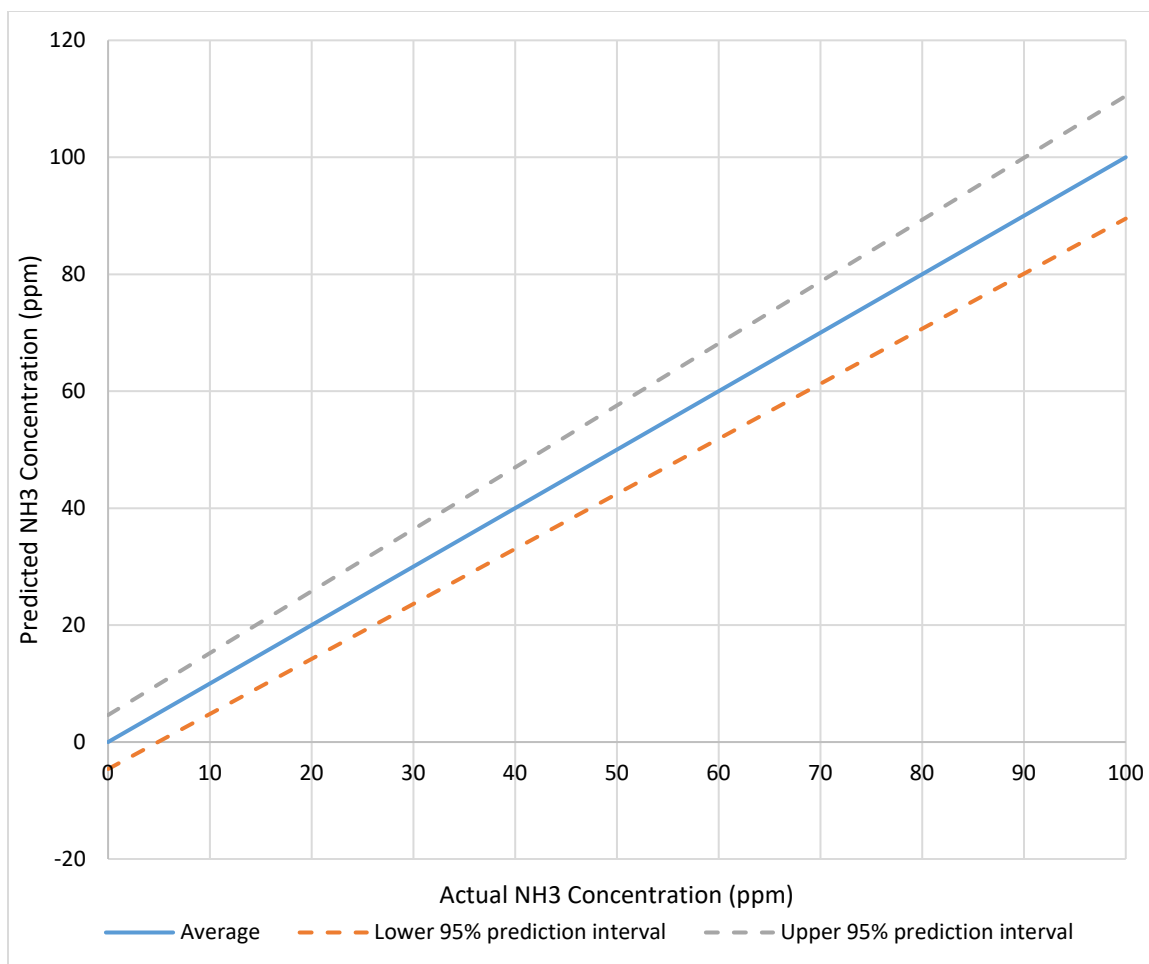


Figure 3-3. Predicted vs actual CH<sub>4</sub> concentration as generated from the two-point calibration.



*Figure 3-4. Predicted vs actual CO<sub>2</sub> concentration as generated from the two-point calibration.*



*Figure 3-5. Predicted vs actual NH<sub>3</sub> concentration as generated by the two-point calibration.*

The chamber purge was initially conducted at a flow rate of 1.5 L CO<sub>2</sub> min<sup>-1</sup>, reaching a steady maximum concentration at around 15 minutes. At this point, the chamber base outlet was sealed using tape to reduce further exchange with ambient air. Concentration recording continued overnight; the change in concentration with respect to time was used to evaluate chamber sealing with no gas flow. Because the inlet was left attached to the gas lines, a negative backpressure was possible, and the tape over the outlet may not have been a perfect seal. However, despite those two artificial deficiencies in chamber sealing, concentration drop was less than 10% over the first hour

of turning off calibration gas flow. This was deemed sufficient for the relatively short deployment time within the CBP to proceed without targeting leaks more specifically.

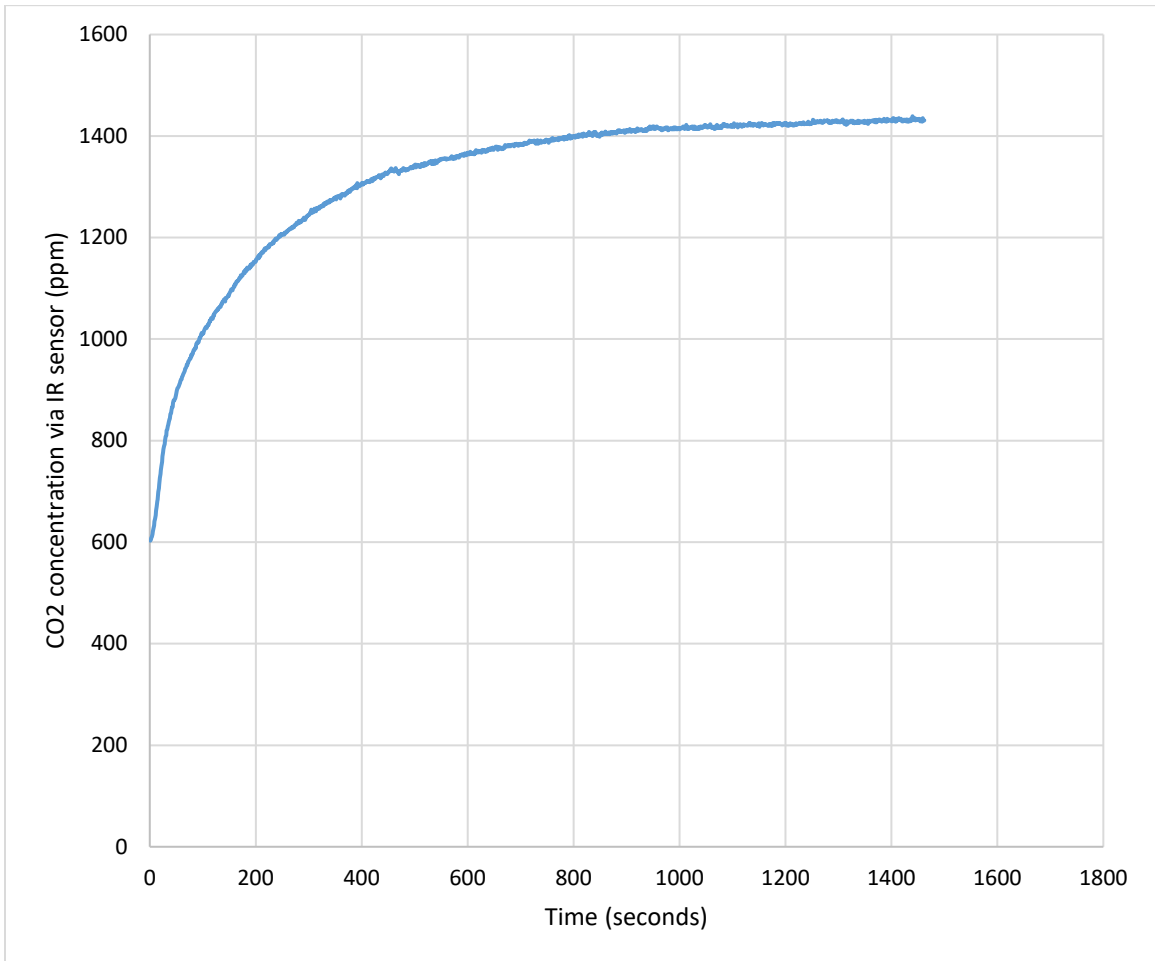


*Figure 3-6. Chamber purge with CO<sub>2</sub>.*

### **3.4. Conclusions**

Calibration resulted in prediction intervals sufficiently small (Figure 3-3, Figure 3-4, and Figure 3-5) to predict relatively small changes in concentration as expected in the CBP barn. Later testing of the NH<sub>3</sub> sensor produced variable zero-gas voltages. The unpredictable drift of the NH<sub>3</sub> sensor made its inclusion problematic; thus, it was determined to use two IR evaluation boards for CH<sub>4</sub> and CO<sub>2</sub> measurement, and obtain values for N<sub>2</sub>O in the field only via gas chromatography.



## **CHAPTER 4: Preliminary CBP Barn Emissions Measurement**

### **4.1. Introduction**

The compost bedded pack barn environment is unique in that it is highly dependent on microbial activity. Maintaining an environment conducive to the typical microbial diversity of the system is not practical in a lab setting; thus, *in situ* testing is necessary. Changes in emissions are expected to be largest immediately after tillage, stabilizing with time. A diurnal trend is not expected because compost temperature is minimally influenced by moderate changes in ambient temperature, and solar radiation is negligible due to the covered facility.

### **4.2. Materials and Methods**

Tests were conducted at the University of Kentucky Coldstream Dairy in the compost bedded pack barn. Tillage of the pack occurs twice each day. The initial measurement occurred over one hour to minimize humidity impacts as recommended in the USDA-ARS GRACEnet protocols (Parkin & Venterea, 2010); after evaluating the first set of data, it was determined that 25 minutes would be a sufficient deployment time to get an accurate concentration curve. Table 4-1 outlines several sampling parameters for the 4 days of data collection. It is important to recognize the impact of the compost moisture content on microbial dynamics and thus gas generation (Maia, 2010); in addition to gas concentration measurements, samples of compost were collected for moisture content analysis.

*Table 4-1. Summary of sampling schemes.*

<b>Date</b>	<b>Tillage</b>	<b>Deployments</b>	<b>MC</b>	<b>GC</b>
June 15	Pre-till	1	46%	CO <sub>2</sub>
June 21	Post-till	1	31%	CO <sub>2</sub> , CH <sub>4</sub> , N <sub>2</sub> O
June 29	Both	3	44-46%	None
July 6	Post-till	3	49%	CO <sub>2</sub> , CH <sub>4</sub> , N <sub>2</sub> O

Prior to the first deployment, the chamber was modified to accommodate manual sampling both to compensate for the unavailable N<sub>2</sub>O sensor and to provide a comparison to a well-established method relative to the electronic sensors. A butyl rubber septum was added to the chamber wall to enable manual withdrawal by syringe. Typically less than 1% of chamber volume was withdrawn in measurements from livestock systems; moreover, the GRACEnet document recommended less than 30 mL of gas removal per sampling time to minimize pressure perturbations. A 20cc syringe was used for gas collection, with manual sampling (Figure 4-1) occurring every 20 minutes to result in four concentration measurements per deployment (t<sub>0</sub>, t<sub>20</sub>, t<sub>40</sub>, t<sub>60</sub>). After each withdrawal, a slight pressure was applied to the syringe plunger as a stopcock was closed to ensure unidirectional outward gas flow until the syringe Luer lock could be sealed, preventing sample dilution with ambient air. Analysis via gas chromatography was conducted in the soil science lab at the University of Kentucky within the 48 hours following sample collection.



*Figure 4-1. Collection setup with the chamber in the CBP.*

### **4.3. Results and Discussion**

In the days prior to field deployment, the chamber purge process was repeated at a lower flow rate (about  $1 \text{ L min}^{-1}$ ) to permit comparison of the known concentration

within the chamber to concentration determined by GC analysis. The primary purpose of this comparison was to provide practice for the method to be used in the field. Samples were withdrawn from the septum in the chamber at 500 second intervals, stored in syringes with stopcocks, and taken to the UK Soil Science Lab for analysis. Precision was determined to be within 5%, as the GC measurements were highly repeatable, initially using 3 injections for each sample. However, in the first two GC sessions, a problem was discovered with sample storage. In comparing the known concentration curve developed by the IR sensor during the chamber purge, the GC readings were low and inconsistent, suggesting diffusion with ambient air. This occurred despite following common recommendations and analyzing samples immediately instead of the “safe” window of 48 hours. The problem was verified after the first field deployment, again with lower than expected concentrations produced by the GC. Storage methods were changed slightly, with the stopcock being replaced by the original needle and now a stopper on the end after sample collection. Analysis of the first samples after implementing the change showed success; all gases showed the expected near-linear increase in concentration with respect to time.

One problem encountered with the CO<sub>2</sub> sensor was a failure to properly process the string of data output by the sensor for a brief period. This problem occurred several times during calibration, but was both unpredictable and infrequent. In the field, the sensor spontaneously resumed correct output and at the expected concentration so as not to cause a significant compromise of data. The rolling 10-point average concentration was used for analysis.

#### 4.3.1. June 15 collection

The first deployment occurred on June 15. Measurement occurred over 1 hour with 20 cc samples withdrawn for GC every 20 minutes starting with  $t = 0$ . Initially a stopcock was used for syringe sealing; analysis later showed that the stopcock was allowing diffusion of ambient air into the syringe, so a rubber stopper was used for subsequent deployments. The shape of the IR CO<sub>2</sub> sensor output showed that by 25 minutes, the CO<sub>2</sub> concentration was approaching an asymptote (Figure 4-2). Since the closed chamber method requires only the initial slope, future deployments were limited to 25-minutes. The CH<sub>4</sub> IR sensor produced inconsistent and primarily unusable values.

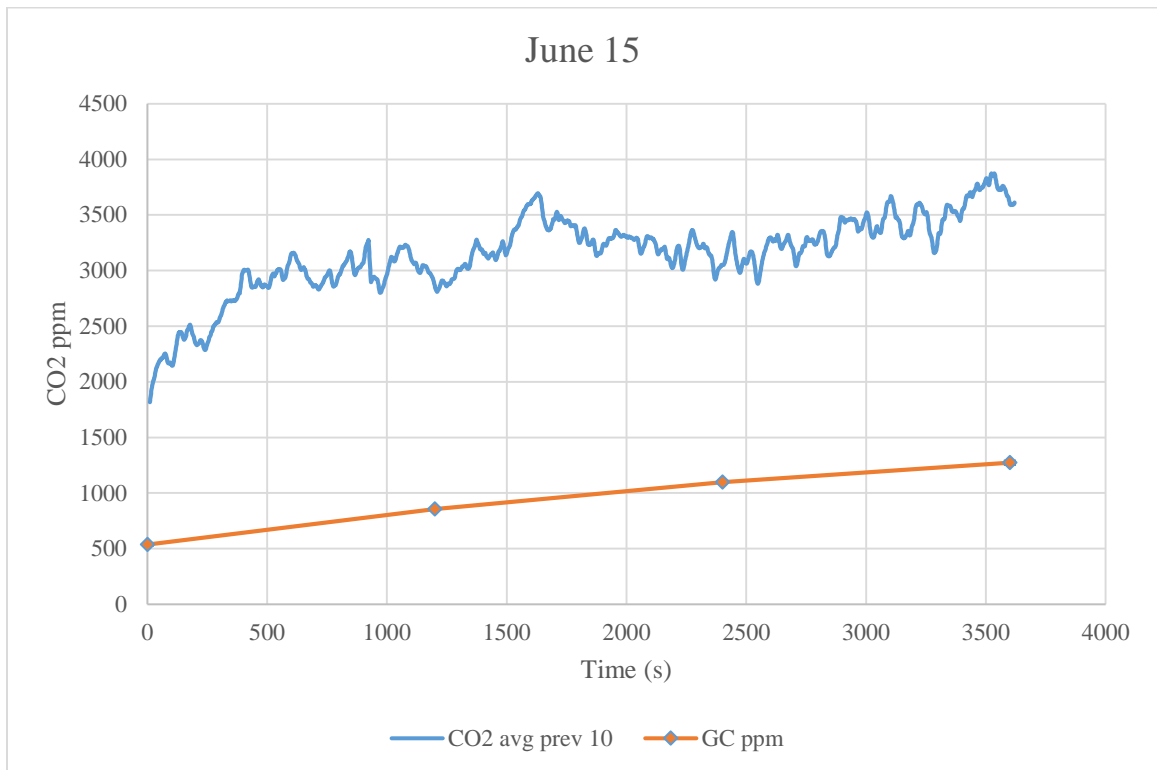


Figure 4-2. June 15 IR and GC measurements.

4.3.2. June 21 collection

The June 21 deployment occurred with very dry compost conditions immediately post-tillage. Samples were collected for GC analysis of CO<sub>2</sub>, CH<sub>4</sub>, and N<sub>2</sub>O. The IR data showed that between the first two GC sample points (t = 0 and t = 500 s), the CO<sub>2</sub> concentration curve could be modeled as linear. In this case, using the 4-point analysis method and weighting towards the second measurement would produce an artificially high initial slope. Concentration curves from both GC and IR are shown in Figure 4-3.

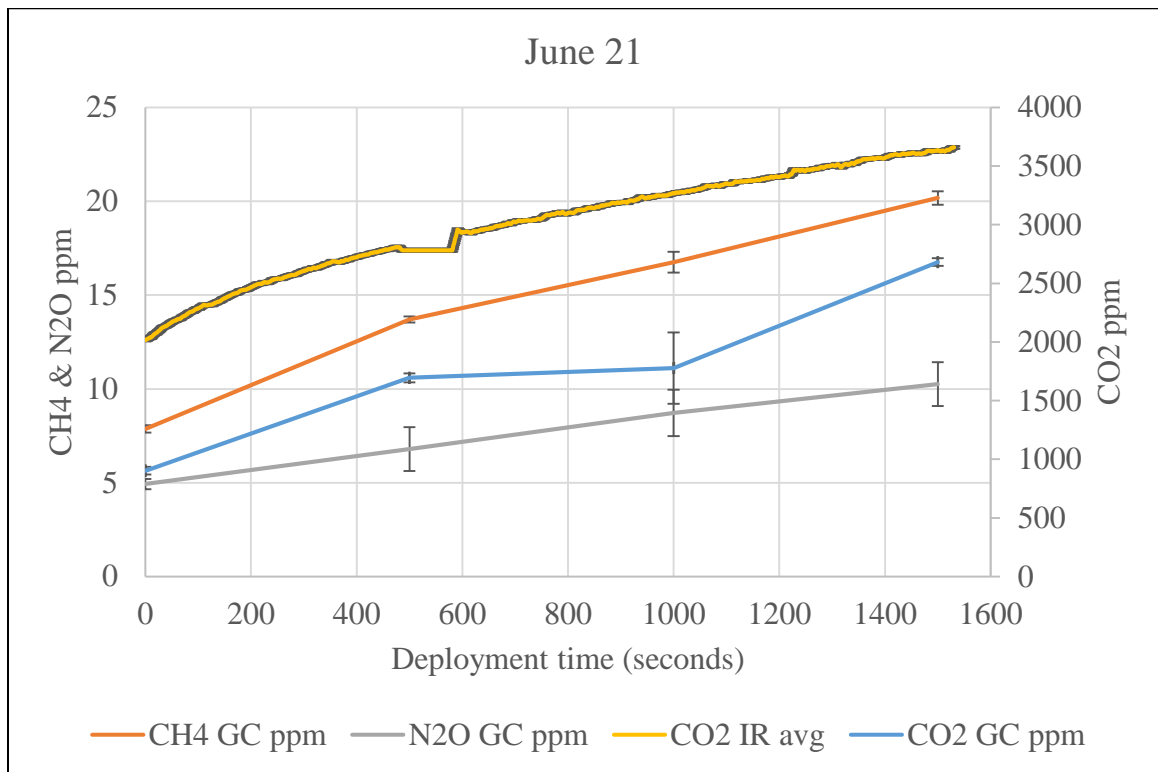


Figure 4-3. June 21 GC and IR data for all gases.

#### 4.3.3. June 29 collection

The June 29 measurements had compost at a fairly average MC. Three 25-minute deployments occurred: one immediately pre-tillage, one 5-30 minutes post-tillage, and one 35-60 minutes post-tillage. Ambient barn concentration data several feet above the pack was also collected, in addition to compost temperatures in areas near the measurement chamber (Table 4-2). The chamber was also allowed to equilibrate to ambient conditions prior to each deployment on the compost surface, resulting in lower CO<sub>2</sub> values which were nearer to normal atmospheric CO<sub>2</sub>. No GC data was collected. IR data for CO<sub>2</sub> across all 3 deployments was similar in shape and values (Figure 4-4).

*Table 4-2. Compost temperature (°C) near the measurement point at various depths.*

Date	Time in relation to tillage	T <sub>surf</sub>	T <sub>10cm</sub>	T <sub>20cm</sub>
June 29	Pre-Tillage	28.5	42.8	52.8
	30 minutes post-tillage	28.0	45.6	46.9
	75 minutes post-tillage	28.0	41.1	45.0
July 6	20 minutes post-tillage	25.2	44.6	46.9
	60 minutes post-tillage	25.0	47.0	48.5
	100 minutes post-tillage	24.8	46.9	49.8

Condensation was visible on the interior of the chamber shell at the end of the second post-tillage deployment due to high pack surface temperature. The increased humidity (Figure 4-5) did not appear to impact the IR sensors.

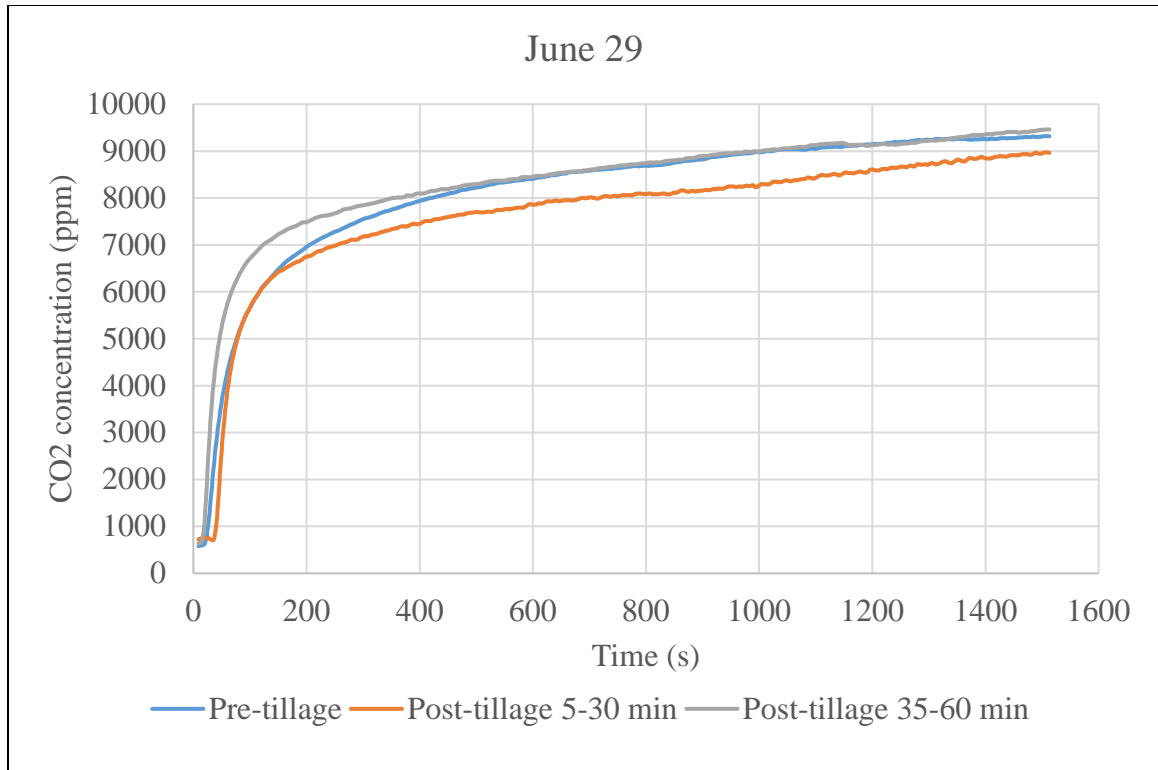
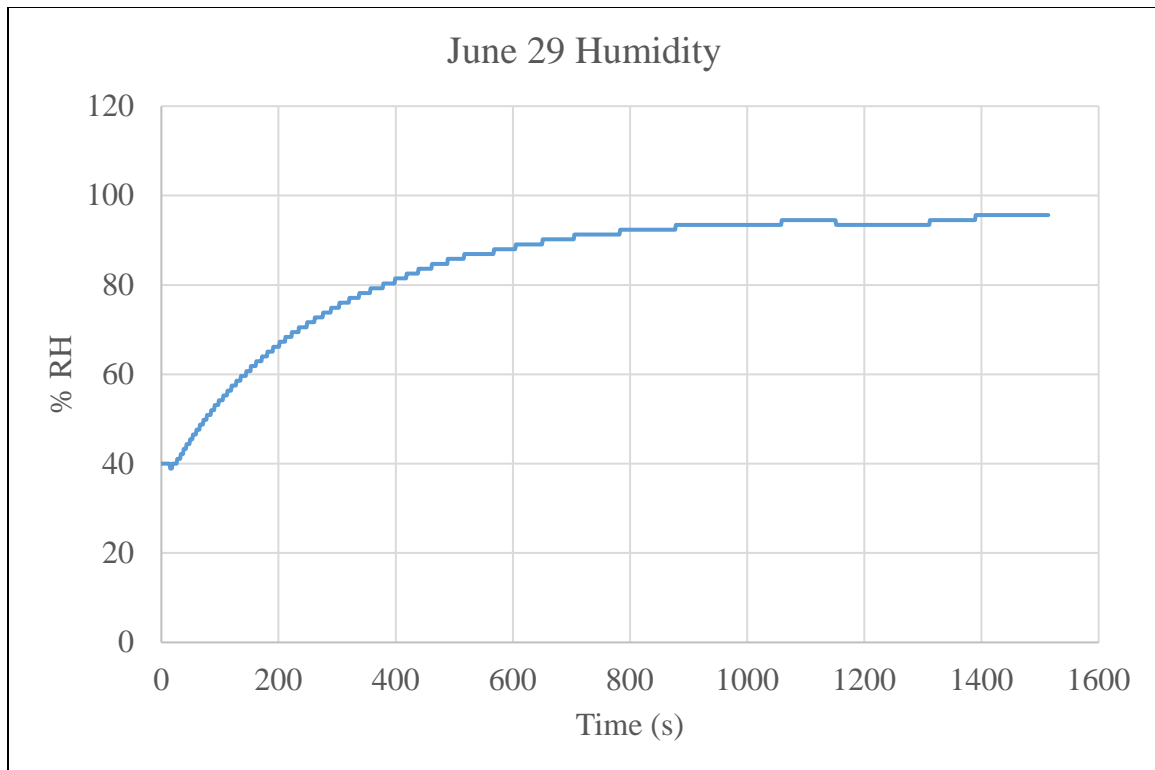


Figure 4-4. June 29 CO<sub>2</sub> data from IR sensor.





*Figure 4-5. June 29 humidity buildup.*

#### 4.3.4. July 6 collection

The July 6 measurements had 3 chamber deployments at 5-30, 35-60, and 65-90 minutes post-tillage. For CO<sub>2</sub> (Figure 4-6) and CH<sub>4</sub> (Figure 4-7), highest emissions occurred immediately after tillage, and lowest in the 35-60 minute period. It is hypothesized that this is the result of gases from the lower compost layers being stirred up, with stabilization occurring during the 65-90 minute period. The gas flux from layers below tillage layer may be contributing the increase in concentration. A fourth deployment post-tillage would provide a better idea of true gas production trends in relation to tillage time. N<sub>2</sub>O fluxes were small, with initial slopes from the 35-60 and 65-90 minute periods not different from zero (Figure 4-8).

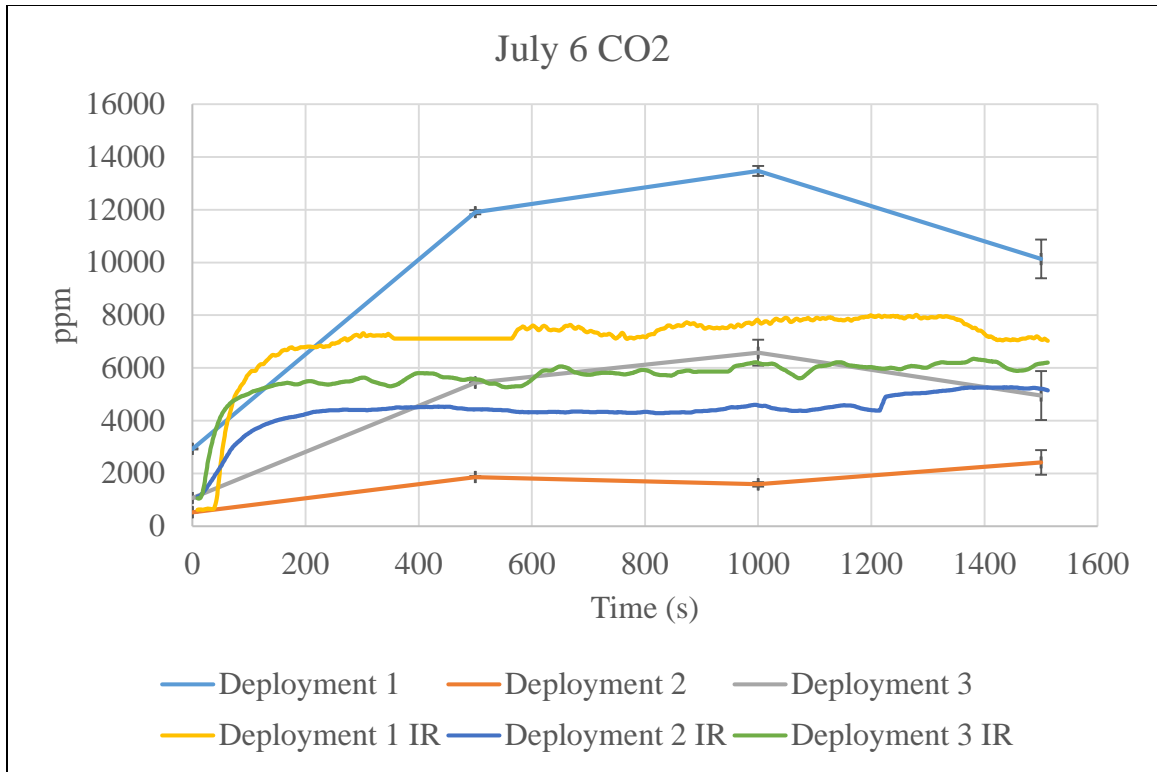


Figure 4-6. July 6 CO<sub>2</sub> from both IR and GC, all deployments.

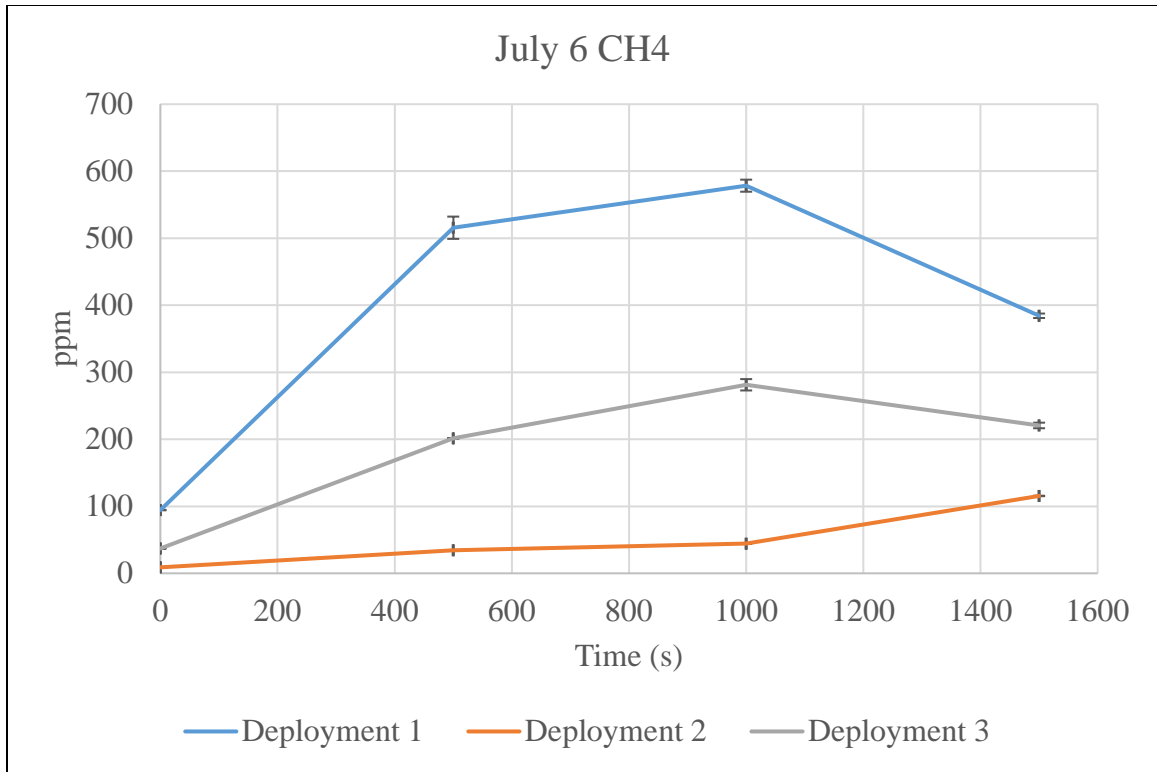


Figure 4-7. July 6 CH<sub>4</sub> from GC.

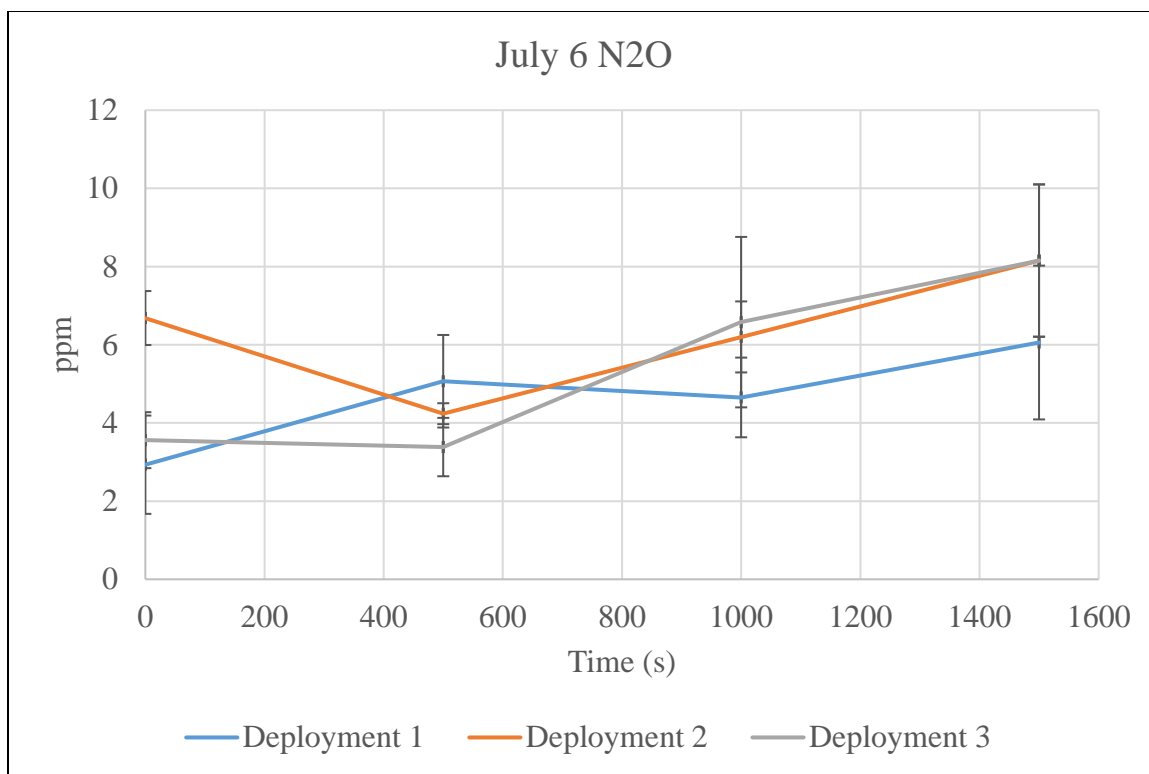


Figure 4-8. July 6 N<sub>2</sub>O from GC.

#### 4.3.5. Analysis of initial slopes

After data collection, the next challenge was determining how to analyze the data. Initially, MATLAB was used to fit a regression curve to the IR data, and use the first value of the derivative of the fitted curve ( $f'(0)$ ) as the initial emission rate. The data followed the expected trend of a decreasing emission rate over time due to the decreasing concentration gradient between the surface and the ambient chamber concentrations within chamber headspace. However, because the GC method produces so few points, the same curve fitting program could not be run. Parkin and Venterea (2010) suggest an algorithm for finding the initial emission rate using so few points; however, the formula is heavily weighted towards a higher rate because a chamber sealing is assumed to not

occur. The IR sensor output showed that the emission rate was approaching an asymptote; thus, some degree of sealing was being achieved and the algorithm when applied to the IR data produced an artificially high emission rate by weighting towards early concentration changes in comparison to the MATLAB fitted curve, which used many points.

In consideration of these problems and noting the comparatively short interval between sample withdrawals, it was decided to use only the first two readings ( $t = 0$  and  $t = 500$  seconds) and assume linearity for the June 21 GC and IR data. However, the same method applied to the June 29 and July 6 data would severely underestimate the slope as the IR sensor demonstrated higher emissions and a more exponential curve shape. Both highlight the importance of obtaining enough data points to estimate the shape of the curve prior to applying fitting.

A possibly useful method for curve fitting comes from Gates et al. 1997

$$C(t) = (C_{equil} - C_0)(1 - e^{-kAt}) + C_0 \quad \text{Equation 4-1}$$

where  $C_{equil}$  is the maximum or equilibrium concentration,  $C_0$  is the minimum or initial concentration,  $A$  is the chamber footprint in m,  $t$  is the time in seconds, and  $k$  is the diffusion coefficient. Comparing the fitted curve to the four “known” points from GC permits  $k$  to be obtained. This procedure allows curve fitting even with relatively few points.

Multiple factors prevented true statistical analysis. First, there were small procedure changes each trip in relation to storage, time since tillage, and ambient data collection. Moreover, with the high spatial and temporal variability of the CBP, statistical comparison of slopes between GC and IR is limited since only one replication could be obtained for each set of conditions. However, simple comparison of individual slopes can still occur for validation of the two methods; the initial slope of for GC and IR, the prediction interval for the CO<sub>2</sub> sensor, and the standard deviation for the GC output was used to compare methods for the June 21 data (Table 4-2). General trends can also be observed as related to tillage and pack moisture content, which could be useful in the design of future sampling schemes using Equation 4-1.

*Table 4-3. Comparison of initial slopes of potential concentration curves obtained via IR and GC (ppm/sec) on June 21.*

IR			GC		
Minimum	Average	Maximum	Minimum	Average	Maximum
1.526	1.531	1.535	1.440	1.584	1.728

*Table 4-4. Gas analysis via GC on June 21.*

Time (seconds)	CO <sub>2</sub>		CH <sub>4</sub>		N <sub>2</sub> O	
	Average ppm	Standard deviation	Average ppm	Standard Deviation	Average ppm	Standard Deviation
0	903	34	8	0.20	5	0.28
500	1695	38	14	0.16	7	1.17
1000	1778	303	17	0.55	9	1.24
1500	2681	33	20	0.36	10	1.16

Concentrations in Table 4-3 were used to determine initial slope in units of ppm/second; this was converted to  $\text{g m}^{-2} \text{h}^{-1}$  using the ideal gas law. The resulting emissions rates are summarized in Table 4-4.

*Table 4-5. Summary of calculated emission rates.*

Date	Deployment	CO <sub>2</sub>	CH <sub>4</sub>	N <sub>2</sub> O
		( $\text{g m}^{-2} \text{h}^{-1}$ )	( $\text{g m}^{-2} \text{h}^{-1}$ )	( $\text{g m}^{-2} \text{h}^{-1}$ )
June 21 (31% MC)	1	1.1	0.0029	0.0027
July 6 (49% MC)	1	100.2	0.21	0.0031
July 6 (49% MC)	2	24.1	0.013	Not significant
July 6 (49% MC)	3	26.4	0.082	Not significant

#### **4.4. Conclusions**

CO<sub>2</sub>, N<sub>2</sub>O, and CH<sub>4</sub> were successfully measured in the CBP. The CO<sub>2</sub> sensor was compared to concentration readings produced via GC and while the concentrations were different in absolute values, the slope of the concentration curves was not different. Thus, the IR sensor successfully measured CO<sub>2</sub> similarly to the GC method. CH<sub>4</sub> and N<sub>2</sub>O values were sufficiently high to be measurable via GC; however, the CH<sub>4</sub> flux was too small to be detected with the calibrated IR sensor over the required measurement period. A N<sub>2</sub>O sensor could not be obtained but a similar result is expected. The chamber can successfully measure CO<sub>2</sub> via IR and allows collection of trace gas samples to be analyzed via GC. The slopes of the concentration curves validate the data because they indicate no leaks occurred. Despite humidity and temperature buildup within the measuring chamber, sensor outputs indicate that high values did not cause any measurement problems over the 25-minute deployment period.



## CHAPTER 5: Conclusions

A chamber was successfully developed to measure emissions specifically from the CBP at a lower cost than commonly used livestock emissions measurement systems. CO<sub>2</sub> emission rate can easily be measured with a similar accuracy to GC and even greater precision. CH<sub>4</sub> and N<sub>2</sub>O emission rates were determined via GC only; CH<sub>4</sub> fluxes were too low to be detected by available IR sensors, and while an N<sub>2</sub>O sensor could not be obtained, the result is expected to be similar. Due to its inconsistent initial value, even in the calibration process, the NH<sub>3</sub> sensor was deemed unreliable for this study.

The problems with sample storage encountered during GC analysis highlight the importance of testing sample storage methods frequently, contributing to the higher labor requirements of traditional GC measurement systems. Further, calculated emissions rate is highly dependent upon the method of slope analysis. Manual sampling for GC analysis provides few points, and thus greater uncertainty of the true concentration curve from which initial emissions rate can be inferred. An accurate CO<sub>2</sub> curve obtained via IR sensor provided guidance as to the true curve type, which also aided in selection of a suitable analysis method for other gases. The importance of oversampling cannot be overstated as it can allow less expensive methods to produce data of comparable or even greater value than traditional systems, especially as the lower cost permits more chambers to be deployed so as to also capture spatial variation within such a heterogeneous system as the CBP.

While only CO<sub>2</sub> could confidently be measured with an IR sensor alone, the hybrid chamber developed would be useful for automated measurements of CBP aerobic respiration and thus pack performance by estimating rate of microbial breakdown of materials; additionally, the measurement chamber provides a relatively inexpensive

enclosure for evaluation of trace gases via the more traditional GC method. In addition, the measurement of chamber humidity and temperature can provide additional information to bed performance. The bed drying rate, or moisture evaporation rate, can be calculated from these environmental measurements. This is an important value for the evaluation of the needed compost resting area per cow for compost bed moisture control and desired compost barn resting area needed for barn dimensions.

Two future research steps are immediately apparent. The first is deployment of multiple chambers within a CBP to capture spatial variation within a system (Figure 5-1). Previously this would be limited by chamber cost; however, the inexpensive chamber developed allows many chambers to be deployed at the same cost as one large traditional chamber. A challenge would be simultaneously initiating all chambers because concentration of gas builds up extremely quickly and a few minutes of setup could alone result in apparently significant emission differences; however, this could likely be corrected with mathematical modeling because only the initial slope matters.

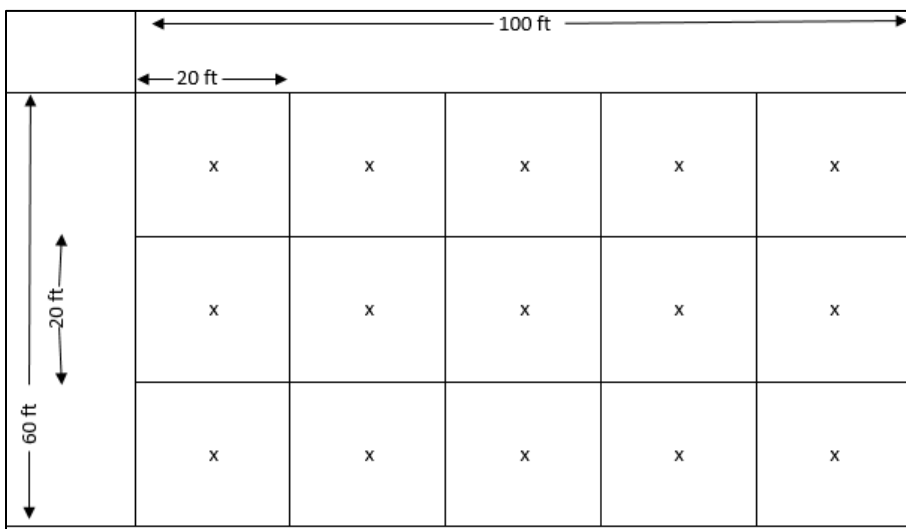


Figure 5-1. Example layout of chambers for sampling entire barn.

The other would be comparison of manure storage methods. The N<sub>2</sub>O emissions from the CBP are significant despite the primarily aerobic surface layer, likely due to coupled nitrification-denitrification as discussed in Chapter 1. However, a comparison would need to occur between manure storage methods before making conclusions about the CBP's environmental impact. Similarly, non-enteric CH<sub>4</sub> would intuitively be lower but an actual comparison should occur. In comparing gas emission ratios to Leytem et al. (2011)'s evaluation of a combination of a large, open dairy lot, the CBP ratio of CO<sub>2</sub> to CH<sub>4</sub> obtained in this study shows a greater proportion of carbon emissions going towards CO<sub>2</sub> (0.00737 g CH<sub>4</sub>/g CO<sub>2</sub> vs 0.0188 g CH<sub>4</sub>/g CO<sub>2</sub>). Upon initial inspection, it appears that N<sub>2</sub>O emission is also proportionately higher (0.00236 g N<sub>2</sub>O/g CO<sub>2</sub> vs 0.000313 g N<sub>2</sub>O/g CO<sub>2</sub>), but too many variables could contribute to this difference; a study investigating N<sub>2</sub>O between manure storage systems should use the same cows to eliminate diet effects. Results from several different studies are shown in Table 5-1.

*Table 5-1. Comparison of emissions across several studies.*

<b>Source</b>	<b>Facility</b>	<b>CO<sub>2</sub> range</b> <b>(g m<sup>-2</sup> h<sup>-1</sup>)</b>	<b>CH<sub>4</sub> range</b> <b>(g m<sup>-2</sup> h<sup>-1</sup>)</b>	<b>N<sub>2</sub>O range</b> <b>(g m<sup>-2</sup> h<sup>-1</sup>)</b>
Leytem et al	Compost	8.5-52.6	0.11-1.5	0.0050-1.11
	Open lots	6.3-41.7	0.076-0.69	0.00014-0.025
Galama et al	CBP	--	0.0061-1.8	0.0014-0.022
Bonifacio et al	Open lots	--	--	0.00056-0.023
	Open lots	--	--	0.00052-0.021
Current study	CBP (31% MC)	1.1	0.0029	0.0027
	CBP (49% MC)	24.1-100.2	0.013-0.21	Not significant

The measurements of emissions found in the present study are on the same order of magnitude as those of previous studies. These results support the method developed within this project, and suggest potential for utilizing the developed chamber and methods in a more thorough sampling scheme moving forward to develop emissions comparisons. The high spatial and temporal variability should drive thorough documentation of test conditions to include moisture content, humidity, temperature, and time in relation to tillage. Due to such wide variations in conditions, emissions rates cannot directly be compared independently; researches should be creative in their experimental design to capture a variety of conditions and possibly develop models to account for the highlighted variables.

## APPENDICES

### Appendix A. drycalcs.m MATLAB script for evaluating drying characteristics of particles.

```
function [] = drycalcs()

% Katie Wolf 08/17/2015
% drycalcs.m - Drying Rates
% Uses Excel file and user inputs to develop water loss rate (g/kgDM/hr) vs
% MCdb plot, estimate "instantaneous" MCs, etc.

% Format for data in Excel:
%   File name can vary.
%   Two sheets, "Sheet1" and "Sheet2"
%       Sheet1 contains data only from csv file created by program for collecting
%       masses from the scales (averaged over 10min periods).
%       Sheet2 contains data entered by hand from start & end of experiment.

% **Order of variables in Excel Sheet2** (copy & paste to guide entry)
% tare
% start mass, no tubes
% start mass, tubes (no air)
% start mass, air
% end mass, air
% end mass, tubes (no air)
% end mass, no tubes
% MCi tare
% MCi start
% MCi end
% MCf tare
% MCf start
% MCf end

clear;clc;

% Pull in Excel data
prompt = 'Enter file name of data (include file extension): ';
str = input(prompt,'s');
trtnum = input('Enter the number of treatments. ');
trtvec = zeros(1,trtnum);
for i = 1:trtnum
    fprintf('Treatment %.0f- ',i);
    prompt = 'Enter the number of scales: ';
    trtvec(i) = input(prompt);
end
halfrange = input('Specify the number of points over which to find deviation & average. ');

filename = str;
masses = xlsread(filename,'Sheet1'); % masses collected/averaged into csv file
endsdata = xlsread(filename,'Sheet2'); % data input by hand to Excel at start/end
X = size(masses);
L = X(1);
col = X(2);
% trtnum was here

% halfrange was here

% Establish time array (minutes)
time = 10.*ones(L,1);
for i = 2:L
    time(i) = time(i-1) + 10;
end

tare = endsdata(1,:);
```

```

msnt = endsdata(2,:); % start mass, no tubes
mst = endsdata(3,:); % start mass, tubes but no air
msa = endsdata(4,:); % start mass, air on
mea = endsdata(5,:); % end mass, air on
met = endsdata(6,:); % end mass, tubes but no air
ment = endsdata(7,:); % end mass, no tubes
mci_t = endsdata(8,:); % MCI tare
mci_s = endsdata(9,:); % MCI start mass
mci_e = endsdata(10,:); % MCI end mass
mcf_t = endsdata(11,:); % MCF tare
mcf_s = endsdata(12,:); % MCF start mass
mcf_e = endsdata(13,:); % MCF end mass
taretrt = datapull(trtnum,trtvec,tare);
msnttrt = datapull(trtnum,trtvec,msnt);
msttrt = datapull(trtnum,trtvec,mst);
msatrtrt = datapull(trtnum,trtvec,msa);
meatrtrt = datapull(trtnum,trtvec,mea);
mettrt = datapull(trtnum,trtvec,met);
menttrt = datapull(trtnum,trtvec,ment);
mci_ttrt = datapull(trtnum,trtvec,mci_t);
mci_strt = datapull(trtnum,trtvec,mci_s);
mci_etrt = datapull(trtnum,trtvec,mci_e);
mcf_ttrt = datapull(trtnum,trtvec,mcf_t);
mcf_strt = datapull(trtnum,trtvec,mcf_s);
mcf_etrt = datapull(trtnum,trtvec,mcf_e);
mci_wb = wetbasis(col,mci_s,mci_e,mci_t);
mcf_wb = wetbasis(col,mcf_s,mcf_e,mcf_t);
mci_wbtrt = wetbasis(trtnum,mci_strt,mci_etrt,mci_ttrt);
mcf_wbtrt = wetbasis(trtnum,mcf_strt,mcf_etrt,mcf_ttrt);

% Combine masses within a treatment
massestrt = zeros(L,trtnum);
for i = 1:L
    scalenum = 1;
    for j = 1:trtnum
        step = 1;
        while step <= trtvec(j)
            massestrt(i,j) = massestrt(i,j) + masses(i,(scalenum+step-1));
            step = step + 1;
        end
        scalenum = scalenum + trtvec(j);
    end
end

% Combines Sheet 2 data for a treatment
function [xtrt] = datapull(trtnum,trtvec,Y)
    xtrt = zeros(1,trtnum);
    scalenum = 1;
    for j = 1:trtnum
        step = 1;
        while step <= trtvec(j)
            xtrt(j) = xtrt(j) + Y(scalenum+step-1);
            step = step + 1;
        end
        scalenum = scalenum + trtvec(j);
    end
end

% Calculates wet basis MCs, both individually and whole treatments
function [mc_wb] = wetbasis(col,mci_s,mci_e,mci_t)
    mc_wb = zeros(1,col);
    for i = 1:col
        mc_wb(i) = (mci_s(i)-mci_e(i))/(mci_s(i)-mci_t(i));
    end
end

% Calculations of "background" data from Sheet 2
mtt = tare + (mst-msnt); % tare plus tubing - mass of everything but material

```

```

mttrt = taretrt + (mstrt-msnttrt);
mat = msnt - tare; % material mass
mattrt = msnttrt - taretrt;
dm = (1-mci_wb).*mat; % dry matter est using MCI
dmtrt = (1-mci_wbtrt).*mattrt;
startwater = mat-dm; % starting water estimate
startwatertrt = mattrt-dmtrt;
waterloss = msnt-ment; % diff between start and end mass for water loss
waterlosstrt = msnttrt-menttrt;
endmass = ment - tare; % end amount of material
endmasstrt = menttrt - taretrt;
endwater = mcf_wb.*endmass; % end amount of water from actual MCF and end material
endwatertrt = mcf_wbtrt.*endmasstrt;

% More involved calculations via functions
change = masschange(L,col,masses);
changetrt = masschange(L,trtnum,massestrt);
waterpres = water(L,col,endwater,change);
waterprestrt = water(L,trtnum,endwatertrt,change);
sumwaterloss = sumwater(col,L,change);
sumwaterlosstrt = sumwater(trtnum,L,changetrt);
rate = dryrate(col,L,change,dm);
ratetr = dryrate(trtnum,L,changetrt,dmtrt);
mcd = drybasis(col,L,waterpres,mat,sumwaterloss);
mcdtrt = drybasis(trtnum,L,waterprestrt,mattrt,sumwaterlosstrt);

filt = filter(rate,col,halfrange);
filttrt = filter(ratetr,trtnum,halfrange);

% avg = averagearray(filt,col,halfrange);
% avgtrt = averagearray(filttrt,trtnum,halfrange);

interp = interpolation(filt,col);
interptrt = interpolation(filttrt,trtnum);

interpavg = averagearray(interp,col,halfrange);
interpavgtrt = averagearray(interptrt,trtnum,halfrange);

% Changes - difference between this mass recording and last one
function [change] = masschange(L,col,masses)
    change = zeros(L-1,col);
    for j = 1:col
        for i = 2:L
            change(i-1,j) = masses(i-1,j)-masses(i,j);
        end
    end
end

% waterpres calculation - works backwards to get current water
function [waterpres] = water(L,col,endwater,change)
    waterpres = zeros(L,col);
    for j = 1:col
        waterpres(L,j) = endwater(j);
        step = 1;
        for i = 1:(L-1)
            waterpres((L-step),j) = waterpres(1+(L-step),j)+change((L-step),j);
            step = step + 1;
        end
    end
end

% sum water loss - total water gone at this point; sums change
function [sumwaterloss] = sumwater(col,L,change)
    sumwaterloss = zeros(L-1,col);
    for j = 1:col
        sumwaterloss(1,j) = change(1,j);
        for i = 2:(L-1)
            sumwaterloss(i,j) = sumwaterloss(i-1,j) + change(i,j);
        end
    end
end

```

```

        end
    end
end

% rate - grams of water lost per hr per kg DM
function [rate] = dryrate(col,L,change,dm)
    rate = zeros(L-1,col);
    for j = 1:col
        for i = 1:(L-1)
            rate(i,j) = (change(i,j)/(10/60))/(dm(j)/1000);
        end
    end
end

% dry basis - gets MCdb at this point
function [mcdB] = drybasis(col,L,waterpres,mat,sumwaterloss)
    mcdB = zeros(L-1,col);
    for j = 1:col
        for i = 1:(L-1)
            mcdB(i,j) = waterpres(i+1,j)/(mat(j)-waterpres(i+1,j)-sumwaterloss(i,j));
        end
    end
end

% ri/ro = sqrt(M/M0)
% calculate ri for each M
% graph M vs ri, ri vs time
% temperature profile? from wet/dry interface location

mci_db = zeros(length(col));
for i = 1:col
    mci_db(i) = (mci_s(i) - mci_e(i))/(mci_e(i) - mci_t(i));
end

do = zeros(length(col));
ro = zeros(length(col));
mceq = zeros(length(col));
ri = zeros(L-1,col);
for j = 1:col
    do(j) = input('Enter particle outer diameter in desired units of output variable. ');
    ro(j) = do(j)/2;
    mceq(j) = mcdB(length(mcdB),j);
    for i = 1:(L-1)
        ri(i,j) = sqrt((mcdB(i,j)-mceq(j))/(mci_db(j)-mceq(j)))*ro(j);
        % ri here can never reach zero until mcdB reaches zero,
        % but mcdB is equilibrium w/air, so ri should be zero at that point
    end
end

% volume wet/volume total
volwet = zeros(size(ri));
volwetfrac = zeros(size(ri));
voltotal = zeros(length(col));
for j = 1:col
    voltotal(j) = (4/3)*pi*(ro(j)^3);
    for i = 1:(L-1)
        volwet(i,j) = (4/3)*pi*(ri(i,j)^3);
        volwetfrac(i,j) = volwet(i,j)/voltotal(j);
    end
end

figure()
plot(volwetfrac,ri)
xlabel('Fraction of Volume Wet')
ylabel('Interface Radius (mm)')
legend('5.6 mm','5.6 mm','3.35 mm','3.35 mm','8.0 mm','8.0 mm','Location','northwest')

```



```

figure()
plot(ri,mcdb)
xlabel('Interface Radius (mm)')
ylabel('Moisture Content (dry basis) average')
legend('5.6 mm','5.6 mm','3.35 mm','3.35 mm','8.0 mm','8.0 mm','Location','northwest')

```

```

figure()
plot(time(2:(length(ri)+1)),ri)
xlabel('Time (min)')
ylabel('Interface Radius (mm)')
legend('5.6 mm','5.6 mm','3.35 mm','3.35 mm','8.0 mm','8.0 mm','Location','northeast')

```

```

% Filtering - uses Median Absolute Deviation to replace outliers with NaN
% (primarily for plotting purposes)

```

```

function [filt] = filter(rate,col,halfrange)
    filt = rate;
    for j = 1:col
        for i = (halfrange+1):(L-halfrange-1) % excludes ends
            samp = rate(i-halfrange:i+halfrange,j);
            sampmed = median(samp);
            sampdev = abs(samp-sampmed);
            sampdevmed = 1.4826*median(sampdev);
            if abs(rate(i,j) - median(samp)) > sampdevmed
                filt(i,j) = NaN;
            else
                filt(i,j) = rate(i,j);
            end
        end
    end
end

```

```

function [avg] = averagearray(filt,col,halfrange)
    avg = filt;
    for j = 1:col
        for i = (halfrange+1):(L-halfrange-1)
            count = 1;
            lowtot = 0;
            hitot = 0;
            while count <= halfrange
                lowtot = lowtot + filt(i-count,j);
                hitot = hitot + filt(i+count,j);
                count = count + 1;
            end
            avg(i,j) = (lowtot + hitot)/(2*halfrange);
        end
    end
end

```

```

% function from MATLAB fileshare to replace NaN in 1D array

```

```

function [x] = repnan(x,method)
% REPANAN replaces NaN values in a 1D array.
%
%% Syntax
%
% x = repnan(x);
% x = repnan(x,method);
%
%% Description
%
% x = repnan(x) returns x sans NaNs.
%
% x = repnan(x,method) specifies a method for replacing the original x's
% NaNs. Methods can be 'nearest', 'linear', 'spline', 'pchip', 'cubic',
% 'v5cubic', 'next', or 'previous'. The 'next' options replaces NaNs with
% the next non-NaN value in x. The 'previous' option replaces NaNs with
% the previous non-NaN value in x. Default is 'linear'.
%

```

```

%% Author Info
%
% Written by Chad A. Greene of the University of Texas at Austin's
% Institute for Geophysics, October 31, 2014. Feel free to visit Chad
% over at http://www.chadagreene.com.
%
% See also: interp1, find, NaN, and isnan.

%% Input check:

assert(isvector(x)==1,'The repnan function requires that x must be a 1D vector.')
```

%% Use linear 1D interpolation by default:

```

if nargin == 1
    method = 'linear';
end

%% Transpose to row vector if necessary:

StartedColumn = false;
if iscolumn(x)
    x = x';
    StartedColumn = true;
end

%% Perform interpolation:

switch lower(method)
    case 'next'
        for k = find(isnan(x))
            try
                x(k) = x(find(1:length(x)>k & isfinite(x),1,'first'));
            end
        end

    case {'last','prev','previous'}
        for k = find(isnan(x))
            try
                x(k) = x(find(1:length(x)<k & isfinite(x),1,'last'));
            end
        end

    case {'linear','cubic','nearest','spline','pchip','v5cubic'}
        x(isnan(x)) = interp1(find(~isnan(x)),x(~isnan(x)),find(isnan(x)),method);

    otherwise
        error('Unrecognized method of interpolation.')
end

%% Recolumnate x if user entered x as a column vector:

if StartedColumn
    x = x';
end

end

% use above function, iterate for each column
function [interp] = interpolation(filt,col)
    interp = zeros(size(filt));
    for j = 1:col
        interp(:,j) = repnan(filt(:,j),'spline');
    end
end

% Plotting
```

```

figure()
plot(mcdb(:,7),filt(:,7),mcdb(:,7),rate(:,7),mcdb(:,7),interp(:,7),mcdb(:,7),interpavg(:,7))
legend('filtered','original','Interpolated','Interpolated w/moving
average','Location','southeast')
xlabel('Moisture Content (dry basis)')
ylabel('Drying Rate (g/kgDM/hr)')
title('Sawdust bedding drying')
% figure()
% plot(mcdb,rate)
% xlabel('MCdb')
% ylabel('Rate')
% legend('5.6 mm','5.6 mm','3.35 mm','3.35 mm','8.0 mm','8.0 mm','Location','northwest')

%
% getting a drying constant, k
% figure()
% plot(time(2:length(mcdb)+1),mcdb)
% % mcdb= MCI*e^(-kt)
% % ln(mcdb/MCI)=-kt

% get k for every point? then average k? apply?

k = zeros(size(mcdb));
for i = 1:length(mcdb)
    for j = 1:col
        k(i,j) = log(mcdb(i,j)/mcdb(1,j))/-time(i+1);
    end
end
kavg = mean(k,1)
kstdev = std(k,1)

expfun = zeros(size(mcdb));
expfunavg = zeros(size(mcdb));
for i = 1:length(mcdb)
    for j = 1:col
        expfun(i,j) = mcdb(1,j)*exp(-k(i,j)*time(i+1));
        expfunavg(i,j) = mcdb(1,j)*exp(-kavg(j)*time(i+1));
    end
end

% for j = 1:col
%     figure()
%     plot(time(2:length(mcdb)+1),mcdb(:,j),time(2:length(mcdb)+1),expfun(:,j),'--
%',time(2:length(mcdb)+1),expfunavg(:,j),'--')
%     title(j)
%     legend('Original','var k','avg k','Location','Northeast')
%     xlabel('Time (min)')
%     ylabel('MCdb')
% end
%
% figure()
% plot(time(2:length(mcdb)+1),k)
% legend('1','2','3','4','5','6')
% xlabel('Time (min)')
% ylabel('k')
%
% for j = 1:col
%     figure()
%     histogram(k(:,j))
% end

% need a way to numerically compare models- is using kavg appropriate?
% H0: MCidb*exp^(-kavg*t)-MCI*exp^(-k*t)=0

```

```

eabs = zeros(size(mcdb));
e = zeros(size(mcdb));
for i = 1:length(mcdb)
    for j = 1:col
        eabs(i,j) = expfun(i,j)-expfunavg(i,j);
        e(i,j) = eabs(i,j)/mcdb(i,j);
    end
end

figure()
plot(time(2:length(mcdb)+1),eabs)
xlabel('time (min)')
ylabel('absolute error of average k')

figure()
plot(time(2:length(mcdb)+1),e)
xlabel('time (min)')
ylabel('relative error of average k')

figure()
plot(mcdb,eabs)
xlabel('MCdb')
ylabel('absolute error of average k')

figure()
plot(mcdb,e)
xlabel('MCdb')
ylabel('relative error of average k')

% ln_mcdb = zeros(size(mcdb));
% for i = 1:length(mcdb)
%     for j = 1:col
%         ln_mcdb(i,j) = log(log(mcdb(i,j)/mcdb(1,j)));
%     end
% end
%
% for j = 1:col
%     figure()
%     plot(time(1:length(mcdb)),ln_mcdb(:,j))
% end

% for j = 1:col
%     figure()
%     histogram(e(:,j))
% end

% plot(mcdb(:,2),filt(:,2),mcdb(:,2),avg(:,2),mcdb(:,2),interp(:,2),mcdb(:,2),interpavg(:,2))
% legend('Filter only','Filter + moving avg','interp','interp avg')

% % Plot mass vs time
% plot(time,masses)
% xlabel('Time (minutes)')
% ylabel('Mass (g)')

% histogram(change)

%*** Items to potentially improve/add***
% Reports- get all scale graphs, treatments, include mass vs time graph, histograms of
% distributions. Too much plotting to do all at once in separate windows
% Export to PDF?
%
% % Derivatives
% % Asks for user input for span over which to calculate slope
% % Can be used to note significant slope changes- potential critical points
%
% % Doesn't work great due to data errors- insignificant changes from + to -
% % derivative.

```

```

%
%% derspan = input('Enter the number of points across which the derivative is to be calculated.
');
%% der = zeros(L-1-derspan,col);
%
%% for j = 1:col
%%     for i = 1:(L-1-derspan)
%%         der(i,j) = (rateaverage(i,j)-rateaverage(i+derspan,j))/(mcdb(i,j)-mcdb(i+derspan,j));
%%     end
%% end
%
%
%% Plotting
%% Decide to plot individually, all on one, or a combination of the two.
%% Should be neater since lots of possible variables
%
%% Currently avg & filtered data only show up for "sep"
prompt = 'Plot scales separately, all on one, or combination? [sep, all, com]';
str = input(prompt,'s');
if strcmpi(str,'sep')
    for j = 1:col
        figure()
        plot(mcdb(:,j),rate(:,j),mcdb(:,j),ratefil(:,j),mcdb(:,j),rateaverage(:,j))
        title(j)
        xlabel('dry basis')
        ylabel('loss of water (g/hr/kgDM)')
        legend('Original','Filtered','Moving Avg','Location','Northwest')
    end
elseif strcmpi(str,'all')
    plot(mcdbtrt,rate)
    title('All')
    xlabel('dry basis')
    ylabel('loss of water (g/hr/kgDM)')
else
    for j = 1:col
        figure()
        plot(mcdb(:,j),rate(:,j))
        title(j)
        xlabel('dry basis')
        ylabel('loss of water (g/hr/kgDM)')
    end
    plot(mcdb,rate)
    title('All')
    xlabel('dry basis')
    ylabel('loss of water (g/hr/kgDM)')
end

% More Potential improvements:

% Get inflection points?

% Using finite sections to estimate derivative by slope not good- errors in
% data screw it up. Look into diff(rateaverage,mcdb) - issue may be
% rateaverage not direct function of mcdb (rearrange?).

% Difference in average of several derivatives?
end

```

## Appendix B. ChamberMeasIR VB.net program for data collection.

```
Imports System.IO.Ports

Public Class Form1
    Dim elapsed As Integer = 0
    Private DAQ As Mccdaq.Mccboard
    Dim AvailPorts As Array
    Delegate Sub settextcallback(ByVal [text] As String)

    Private Sub Form1_Load(ByVal sender As Object, e As EventArgs) Handles MyBase.Load

        CheckForIllegalCrossThreadCalls = False
        DAQ = New MccDaq.MccBoard(0)
        BoardNameTextBox.Text = DAQ.BoardName

        AvailPorts = SerialPort.GetPortNames()
        co2PortSelect.Items.AddRange(AvailPorts)
        ch4PortSelect.Items.AddRange(AvailPorts)
        Timer.Enabled = True

    End Sub

    Private Sub co2Open_Click(sender As Object, e As EventArgs) Handles co2Open.Click
        If co2Port.IsOpen = False Then
            co2Port.PortName = co2PortSelect.Text
            co2Port.BaudRate = 9600
            co2Port.DataBits = 8
            co2Port.StopBits = StopBits.One
            co2Port.Parity = Parity.None
            co2Port.Handshake = Handshake.None
            co2Port.ReadTimeout = 999
            co2Port.Open()
            co2Open.Text = "Disconnect"
        Else
            co2Port.Close()
            co2Open.Text = "Connect"
        End If
        ' Continue to write until response is recieved
        ' After initial command sent, IR board automatically responds every second
        While co2OutputTextBox.Text = ""
            co2Port.Write("[EK2 SEN MEA]")
            co2OutputTextBox.Text = co2Port.ReadLine
        End While
        Timer.Enabled = True
    End Sub

    Private Sub ch4Open_Click(sender As Object, e As EventArgs) Handles ch4Open.Click
        If ch4Port.IsOpen = False Then
            ch4Port.PortName = ch4PortSelect.Text
            ch4Port.BaudRate = 9600
            ch4Port.DataBits = 8
            ch4Port.StopBits = StopBits.One
            ch4Port.Parity = Parity.None
            ch4Port.Handshake = Handshake.None
            ch4Port.ReadTimeout = 999
            ch4Port.Open()
            ch4Open.Text = "Disconnect"
        Else
            ch4Port.Close()
            ch4Open.Text = "Connect"
        End If
        ' Continue to write until response is recieved
        ' After initial command sent, IR board automatically responds every second
        While ch4OutputTextBox.Text = ""
            ch4Port.Write("[EK2 SEN MEA]")
            ch4OutputTextBox.Text = ch4Port.ReadLine
        End While
    End Sub
End Class
```

```

End While
Timer.Enabled = True
End Sub

Private Sub Timer_Tick(sender As Object, e As EventArgs) Handles Timer.Tick
    ' DAQ Board:
    Dim Status0 As MccDaq.ErrorInfo
    Dim Status1 As MccDaq.ErrorInfo
    Dim Status2 As MccDaq.ErrorInfo
    Dim TempVolt As Double
    Dim HumidityVolt As Double
    Dim nh3Volt As Double
    DAQ.AInputMode(MccDaq.AInputMode.Differential) 'DAQ.BoardConfig.SetNumAdChans(4)
    DAQ.BoardConfig.SetAIChanType(0, MccDaq.AIChanType.Voltage)
    DAQ.BoardConfig.SetAIChanType(1, MccDaq.AIChanType.Voltage)
    DAQ.BoardConfig.SetAIChanType(2, MccDaq.AIChanType.Voltage)
    Status0 = DAQ.VIn32(0, MccDaq.Range.Bip5Volts, TempVolt, MccDaq.VInOptions.Default)
    Status1 = DAQ.VIn32(1, MccDaq.Range.Bip5Volts, HumidityVolt, MccDaq.VInOptions.Default)
    Status2 = DAQ.VIn32(2, MccDaq.Range.BipPt078Volts, nh3Volt, MccDaq.VInOptions.Default)
    StatusTextBox.Text = Status0.Message & "," & Status1.Message & "," & Status2.Message
    TempVoltTextBox.Text = Format(TempVolt, "#0.00")
    HumidityVoltTextBox.Text = Format(HumidityVolt, "#0.000")
    nh3Volt = nh3Volt * 1000 ' conversion V to mV
    nh3VoltTextBox.Text = Format(nh3Volt, "0.000")
    ' TempTextBox.Text = Format(TempVolt * 10, "#.0") ' eventual temperature conversion from
voltage to Celsius
    ' HumidityTextBox.Text = Format(HumidityVolt * 200, "#.0") ' eventual RH conversion from
voltage to %
    nh3TextBox.Text = Format(nh3Volt * 781.9681 - 62.1769, "#0.") ' NH3 conversion from mV to
ppm

    If co2Port.IsOpen Then
        Dim co2Output As String = co2Port.ReadExisting
        Dim co2OutputTrimmed As String = co2Output.TrimStart
        co2OutputTextBox.Text = co2OutputTrimmed
        If co2OutputTextBox.Text.Length = 53 Then
            Dim checkstart1 As String = co2OutputTextBox.Text.Substring(0, 4)
            If checkstart1 = "[EK2" Then
                Dim co2RefH As String = co2OutputTextBox.Text.Substring(9, 4)
                Dim co2Ref As Integer = Convert.ToInt32(co2RefH, 16)
                co2RefTextBox.Text = Format(co2Ref * 2.048 / 65535, "0.000000")
                co2TempTextBox.Text = co2OutputTextBox.Text.Substring(40, 5) ' deg C
                Dim co2BulbH As String = co2OutputTextBox.Text.Substring(46, 4)
                Dim co2Bulb As Integer = Convert.ToInt32(co2BulbH, 16)
                co2BulbTextBox.Text = Format(co2Bulb * 2.048 / 65535, "0.000000")
                Dim co2ActH As String = co2OutputTextBox.Text.Substring(19, 4)
                Dim co2Act As Integer = Convert.ToInt32(co2ActH, 16)
                co2ActTextBox.Text = Format(co2Act * 2.048 / 65535, "0.000000")
                Dim co2zerocalc As Single = 0.288
                Dim co2spancalc As Single = 0.9249
                Dim co2nr As Single = (co2ActTextBox.Text / (co2zerocalc *
co2RefTextBox.Text))
                Dim co2Conc As Single = (Math.Log(1 - ((1 - co2nr) / co2spancalc))) * -10000
                co2ConcTextBox.Text = Format(co2Conc, "0.")
            End If
        End If
    End If

    If ch4Port.IsOpen Then
        Dim ch4Output As String = ch4Port.ReadExisting
        Dim ch4OutputTrimmed As String = ch4Output.TrimStart
        ch4OutputTextBox.Text = ch4OutputTrimmed
        If ch4OutputTextBox.Text.Length = 53 Then
            Dim checkstart2 As String = ch4OutputTextBox.Text.Substring(0, 4)
            If checkstart2 = "[EK2" Then
                Dim ch4RefH As String = ch4OutputTextBox.Text.Substring(9, 4)
                Dim ch4Ref As Integer = Convert.ToInt32(ch4RefH, 16)
                ch4RefTextBox.Text = Format(ch4Ref * 2.048 / 65535, "0.000000")
                ch4TempTextBox.Text = ch4OutputTextBox.Text.Substring(40, 5) ' deg C
            End If
        End If
    End If

```

```

        Dim ch4BulbH As String = ch4OutputTextBox.Text.Substring(46, 4)
        Dim ch4Bulb As Integer = Convert.ToInt32(ch4BulbH, 16)
        ch4BulbTextBox.Text = Format(ch4Bulb * 2.048 / 65535, "0.000000")
        Dim ch4ActH As String = ch4OutputTextBox.Text.Substring(14, 4)
        Dim ch4Act As Integer = Convert.ToInt32(ch4ActH, 16)
        ch4ActTextBox.Text = Format(ch4Act * 2.048 / 65535, "0.000000")
        Dim ch4zerocalc As Single = 2.137619
        Dim ch4spancalc As Single = -0.06257
        Dim ch4nr As Single = (ch4ActTextBox.Text / (ch4zerocalc *
ch4RefTextBox.Text))
        Dim ch4Conc As Single = (Math.Log(1 - ((1 - ch4nr) / ch4spancalc))) * -10000
        ch4ConcTextBox.Text = Format(ch4Conc, "0.")
    End If
End If
End If

If LogButton.Text = "Stop Logging" Then
    Try
        My.Computer.FileSystem.WriteAllText(SaveFileDialog.FileName,
My.Computer.Clock.LocalTime.ToString & "," & co2RefTextBox.Text & "," & co2ActTextBox.Text & "," &
co2ConcTextBox.Text & "," & co2TempTextBox.Text & "," & co2BulbTextBox.Text & "," &
ch4RefTextBox.Text & "," & ch4ActTextBox.Text & "," & ch4ConcTextBox.Text & "," &
ch4TempTextBox.Text & "," & ch4BulbTextBox.Text & "," & nh3VoltTextBox.Text & "," &
nh3TextBox.Text & "," & TempVoltTextBox.Text & "," & TempTextBox.Text & "," &
HumidityVoltTextBox.Text & "," & HumidityTextBox.Text & "," & vbCrLf, True)
        TimeLogging.Enabled = True

    Catch ex As Exception
    End Try
End If
End Sub

Private Sub co2Port_DataReceived(ByVal sender As Object, ByVal e As
SerialDataReceivedEventArgs)
    Dim co2ReceivedText As String
    co2ReceivedText = co2Port.ReadLine
End Sub

Private Sub co2ReceivedText(ByVal [text] As String)
    If co2OutputTextBox.InvokeRequired Then
        Dim x As New settextcallback(AddressOf co2ReceivedText)
        Invoke(x, New Object() {(text)})
    Else
        co2OutputTextBox.Text &= [text]
    End If
End Sub

Private Sub ch4Port_DataReceived(ByVal sender As Object, ByVal e As
SerialDataReceivedEventArgs)
    Dim ch4ReceivedText As String
    ch4ReceivedText = ch4Port.ReadLine
End Sub

Private Sub ch4ReceivedText(ByVal [text] As String)
    If ch4OutputTextBox.InvokeRequired Then
        Dim x As New settextcallback(AddressOf ch4ReceivedText)
        Invoke(x, New Object() {(text)})
    Else
        ch4OutputTextBox.Text &= [text]
    End If
End Sub

Private Sub LogButton_Click(sender As Object, e As EventArgs) Handles LogButton.Click
    If LogButton.Text = "Start Logging" Then
        Try
            SaveFileDialog.ShowDialog()
            My.Computer.FileSystem.WriteAllText(SaveFileDialog.FileName, "Time,C02 ref pk-
pk,C02 act pk-pk,C02 ppm,C02 sensor Temperature (C), C02 bulb pk-pk,CH4 ref pk-pk,CH4 act pk-

```



```

pk,CH4 ppm,CH4 sensor Temperature (C), CH4 bulb pk-pk,NH3 Voltage (mV),NH3 ppm, Temperature
voltage (V),Temperature (C),Humidity Voltage (V),Humidity (% RH)" & vbCrLf, False)
    LogButton.Text = "Stop Logging"
    TimeLogging.Enabled = True
    TimeLogging.Start()

    Catch ex As Exception

    End Try
Else
    LogButton.Text = "Start Logging"
    TimeLogging.Stop()
    elapsed = 0
End If
End Sub

Private Sub TimeLogging_Tick(sender As Object, e As EventArgs) Handles TimeLogging.Tick
    elapsed = elapsed + 1
    TimeLoggingTextBox.Text = elapsed
End Sub
End Class

```

## Appendix C. Supplementary program for use during calibration to write values to the evaluation boards.

```
Imports System.IO.Ports

Public Class Form1

    Dim AvailPorts As Array
    Delegate Sub settexitcallback(ByVal [text] As String)

    Private Sub Form1_Load(ByVal sender As Object, e As EventArgs) Handles MyBase.Load
        CheckForIllegalCrossThreadCalls = False

        AvailPorts = SerialPort.GetPortNames()
        PortSelect.Items.AddRange(AvailPorts)

    End Sub

    Private Sub ConnectButton_Click(sender As Object, e As EventArgs) Handles ConnectButton.Click
        If SerialPort1.IsOpen = False Then
            SerialPort1.PortName = PortSelect.Text
            SerialPort1.BaudRate = 9600
            SerialPort1.DataBits = 8
            SerialPort1.StopBits = StopBits.One
            SerialPort1.Parity = Parity.None
            SerialPort1.Handshake = Handshake.None
            SerialPort1.ReadTimeout = 999
            SerialPort1.Open()
            ConnectButton.Text = "Disconnect"
        Else
            SerialPort1.Close()
            ConnectButton.Text = "Connect"
        End If
    End Sub

    Private Sub SendButton_Click(sender As Object, e As EventArgs) Handles SendButton.Click
        SerialPort1.Write(WriteBox.Text)
        ReadBox.Text = SerialPort1.ReadExisting
    End Sub
End Class
```

## Appendix D. chambhum.m MATLAB script to evaluate time to excessive humidity in chamber.

```

% chambhum.m - 5/30/2017
% Evaluate increase in chamber humidity w.r.t. time to determine
% appropriate deployment time

% inputs Tsurf, Tamb, RHambi, A, V, parameters for DR calc

clear;clc;
close all

Tsurf = 273.15 + input('Enter the pack surface temperature. '); % Kelvin
Tamb = 273.15 + input('Enter the ambient temperature. '); % Kelvin
RHamb = input('Enter the initial ambient humidity (RH, 0-100). ');
A = .1; % chamber footprint (m^2);
V = .0054; % chamber volume (m^3);

WS = 2; % mph
CF = 1;

patm = 101325; % Pa

% calculating surface conditions, assumed constant:
if Tsurf <= 273.16 % is T within specified range for this equation
    psatsurf=exp(31.9602-(6270.3605/Tsurf)-(.46057*log(Tsurf))); % getting lower saturation
    pressure
elseif Tsurf >= 273.16 && Tsurf <= 533.16 % is T within range for this equation
    psatsurf=22105649.25*exp((-27405.526+(97.5413*Tsurf)+(-
    .146244*(Tsurf^2))+(.00012558*(Tsurf^3))+((- .48502*10^-7)*(Tsurf^4)))/((4.34903*Tsurf)-
    (.0039381*(Tsurf^2)))); % getting upper saturation pressure
else % Tdb is out of range for either equation - have user re-check or give up because this won't
    work
    fprintf('The entered dry bulb temperature is out of range.')
end
pvapsurf = 1*psatsurf; % Pa
Hsurf = .6219*pvapsurf/(patm-pvapsurf); % kg H2O/kg dry air, humidity
vsasurf = 287*Tsurf/(patm-pvapsurf); % specific volume surface air
conch20surf = Hsurf/vsasurf; % kg H2O/m^3 air

% saturation pressure calculation
if Tamb <= 273.16 % is T within specified range for this equation
    psatamb=exp(31.9602-(6270.3605/Tamb)-(.46057*log(Tamb))); % getting lower saturation pressure
elseif Tamb >= 273.16 && Tamb <= 533.16 % is T within range for this equation
    psatamb=22105649.25*exp((-27405.526+(97.5413*Tamb)+(-
    .146244*(Tamb^2))+(.00012558*(Tamb^3))+((- .48502*10^-7)*(Tamb^4)))/((4.34903*Tamb)-
    (.0039381*(Tamb^2)))); % getting upper saturation pressure
else % Tdb is out of range for either equation - have user re-check or give up because this won't
    work
    fprintf('The entered dry bulb temperature is out of range.')
end

time = 60*input('Enter the max minutes for chamber deployment. '); % seconds
t = 1:1:time;
RH = zeros(time,1);
RH(1) = RHamb; % percent

pvapamb = zeros(time,1); % Pa
pvapamb(1) = RHamb*psatamb/100;
Hamb = zeros(time,1); % kg H2O/kg dry air, humidity
Hamb(1) = .6219*pvapamb(1)/(patm-pvapamb(1));
vsa = zeros(time,1); % specific volume chamber air - changes slightly w.r.t. time
vsa(1) = 287*Tamb/(patm-pvapamb(1));
conch20amb = zeros(time,1); % kg H2O/m^3 air
conch20amb(1) = Hamb(1)/vsa(1);
DDF = zeros(time,1); % drying driving force = concentration diff
DDF(1) = (conch20surf-conch20amb(1))*2.2*((9.81/32.2)^3);
DR = zeros(time,1); % drying rate, units? kg/(m^2*day)?

```

```

DR(1) = (793.5+27.028*((WS*CF*1.61)^.5)*(((Tamb-273.15)*(9/5)+32)+460)^.67))*DDF(1);
dm = zeros(time,1); % water movement to headspace over time interval
dm(1) = DR(1)*A*(1/3600)/24;
timesat = 1; % starting count for time to saturation (if saturation happens)

for i = 2:time
    DDF(i) = (concH2Osurf-concH2Oamb(i-1))*2.2*((9.81/32.2)^3); % converted from kg H2O/m^3 dry
    air to lb H2O/ft^3 dry air
    DR(i) = (793.5+27.028*((WS*CF*1.61)^.5)*(((Tamb-273.15)*(9/5)+32)+460)^.67))*DDF(i); %
    presumably lb/(ft^2*day)?
    dm(i) = DR(i)*A*(1/3600)/24;
    concH2Oamb(i) = concH2Oamb(i-1)+dm(i)/V;
    Hamb(i) = concH2Oamb(i)*vsa(i-1); % saturates rapidly
    pvapamb(i) = (.6219/Hamb(i))*(1/patm)^(-1);
    vsa(i) = 287*Tamb/(patm-pvapamb(i));
    RH(i) = 100*pvapamb(i)/psatamb;
    if RH(i) < 100
        timesat = timesat + 1;
    end
end

display(timesat)

figure()
plot(t,concH2Oamb)
xlabel('Time, seconds')
ylabel('Abs humidity, kg H2O/m^3')

figure()
plot(t,DDF)
xlabel('Time, seconds')
ylabel('Drying driving force')

figure()
plot(t,DR)
xlabel('Time, seconds')
ylabel('Drying rate')

figure()
plot(t,Hamb)
xlabel('Time, seconds')
ylabel('Humidity ratio, mass H2O/mass dry air')

figure()
plot(t,pvapamb)
xlabel('Time, seconds')
ylabel('Partial vapor pressure, Pa')

figure()
plot(t,RH)
xlabel('Time, seconds')
ylabel('Relative humidity, %')

figure()
plot(t,vsa)
xlabel('Time, seconds')
ylabel('Specific volume, m^3/kg')

```

## Appendix E. ssfind.m MATLAB script to find steady-state values for IR sensor calibration.

```
% ssfind.m 03/01/2017 Katie Wolf
% Finds "steady-state" of voltage output for increasing/decreasing gas
% concentration, allowing calibration.

% Potential improvements:
% post calibration, use average span, zero, testfact?
% evaluate multiple options, choose lowest RMSE?

clear;clc;
close all

% File generated during span calibration (i.e. 1500ppm CO2 for CO2 sensor)
prompt = 'Enter file name of span calibration (include file extension): ';
sfile = input(prompt, 's');

% File generated during zero calibration (i.e. any calibration gas with 0%
% of gas of interest for current calibration)
prompt = 'Enter file name of zero calibration (include file extension): ';
zfile = input(prompt, 's');

avgpts = input('Enter number of points to use in averaging: '); % suggested 10
error = input('Enter maximum allowable error: '); % suggested 10^-4

sdata = xlsread(sfile);
zdata = xlsread(zfile);

svref = sdata(:,1); % reference voltage for span calibration
svact = sdata(:,3); % active channel voltage for span calibration (decreases with increasing
concentration)
sTir = sdata(:,6); % temperature measured by IR sensor during span calibration

zvref = zdata(:,1); % reference voltage for zero calibration
zvact = zdata(:,3); % active channel voltage for zero calibration (maximizes near zero)
zTir = zdata(:,6);

sdvdt = ones(length(sdata),1); % array for differences calculations for span gas
sdvdtavg = ones(length(sdata),1); % array for average of differences for span gas

zdvdt = ones(length(zdata),1); % array for differences calculations for zero gas
zdvdtavg = ones(length(zdata),1); % array for average of differences for zero gas

% Evaluating change in voltage relative to local average:
for i = 2:length(sdata) % span gas file
    sdvdt(i) = (svact(i)-svact(i-1))/((svact(i)+svact(i-1))/2); % essentially percent difference
    if i < avgpts % while not enough previous points to average, use single point
        sdvdtavg(i) = sdvdt(i);
    else
        sdvdtavg(i) = mean(sdvdt(i-(avgpts-1):i)); % average of user-selected # of previous
differences
    end
end

for i = 2:length(zdata) % similar process with zero gas file
    zdvdt(i) = (zvact(i)-zvact(i-1))/((zvact(i)+zvact(i-1))/2);
    if i < avgpts
        zdvdtavg(i) = zdvdt(i);
    else
        zdvdtavg(i) = mean(zdvdt(i-(avgpts-1):i));
    end
end

% Flip array to count points from end to label as steady state
sdevflip = flipud(sdvdtavg);
```

```

sdevcheck = sdevflip(1);
scountback = 1; % initializing count for steady-state determination

% Checking if error small enough to consider steady-state (if "large,"
% steady-state period ends)
while abs(sdevcheck) < error
    sdevcheck = sdevflip(scountback);
    scountback = scountback + 1;
end

% Repeat process for zero gas:
zdevflip = flipud(zdvdtavg);
zdevcheck = zdevflip(1);
zcountback = 1;

while abs(zdevcheck) < error
    zdevcheck = zdevflip(zcountback);
    zcountback = zcountback + 1;
end

% Averaging over steady state period
svrefcal = mean(svref(end-scountback+1:end));
svactcal = mean(svact(end-scountback+1:end));
sTircal = mean(sTir(end-scountback+1:end));

zvrefcal = mean(zvref(end-zcountback+1:end));
zvactcal = mean(zvact(end-zcountback+1:end));
zTircal = mean(zTir(end-zcountback+1:end));

a = 1.01; % per SGX - changes with sensor - create array to allow selection?
n = 1; % .675 per SGX, 1 per calibration
alpha = 0.0005; % per SGX
beta = 0.3; % per SGX
zerocal = zvactcal/zvrefcal;
spancal = (1-svactcal/(zerocal*svrefcal))/(1-exp(-a*(1500/10000)^n));

sNRcomp = ones(1,length(sdata));
sspancomp = ones(1,length(sdata));
sconc = ones(1,length(sdata));

zNRcomp = ones(1,length(zdata));
zspancomp = ones(1,length(zdata));
zconc = ones(1,length(zdata));

% arrays for storage of timestep value
stime = 1:1:length(sdata);
ztime = 1:1:length(zdata);

% Calculating concentrations
for i = 1:length(stime)
    sNRcomp(i) = (svact(i)/(zerocal*svref(i)))*(1+alpha*(sTir(i)-sTircal));
    sspancomp(i) = spancal+(beta*(sTir(i)-sTircal)/sTircal);
    sconc(i) = (-log(1-((1-sNRcomp(i))/sspancomp(i))))/a)*(1/n)*10000;
end

for i = 1:length(ztime)
    zNRcomp(i) = (zvact(i)/(zerocal*zvref(i)))*(1+alpha*(zTir(i)-zTircal));
    zspancomp(i) = spancal+(beta*(zTir(i)-zTircal)/zTircal);
    zconc(i) = (-log(1-((1-zNRcomp(i))/zspancomp(i))))/a)*(1/n)*10000;
end

% finding average calculated concentration
if scountback < zcountback
    sendavg = mean(sconc(end-scountback+1:end));
    zendavg = mean(zconc(end-scountback+1:end));
else
    sendavg = mean(sconc(end-zcountback+1:end));
    zendavg = mean(zconc(end-zcountback+1:end));
end

```

```

% Times required to reach steady-state:
stimes = length(sdata)-scountback;
ztimes = length(zdata)-zcountback;

% Curve fitting:
% Function of time, concentration difference, volume of air lines, flow
% rate. Evaluate min/max to see where constant dC/dt starts; trim.

[SM,SI] = min(sconc);
strimtime = 0:1:(length(sdata)-SI);
strimconc = sconc(SI:end);

[ZM,ZI] = max(zconc);
ztrimtime = 0:1:(length(zdata)-ZI);
ztrimconc = zconc(ZI:end);

fprintf('Time to steady-state is %d s for span trial, %d s for zero trial. \n',stimes,ztimes)

figure()
plot(stime,sconc)
title('Predicted CO2 in 1500ppm CO2 gas')
xlabel('Time (s)')
ylabel('Concentration (ppm)')
figure()
plot(ztime,zconc)
title('Predicted CO2 in CH4 gas')
xlabel('Time (s)')
ylabel('Concentration (ppm)')
figure()
plot(strimtime,strimconc)
title('Trimmed Span Data')
xlabel('Time (s)')
ylabel('Concentration (ppm)')
figure()
plot(ztrimtime,ztrimconc)
title('Trimmed Zero Data')
xlabel('Time (s)')
ylabel('Concentration (ppm)')

```

## Appendix F. ssfindec.m MATLAB script to find steady-state values for electrochemical sensor calibration.

```
% ssfindec.m 03/16/2017 Katie Wolf
% Finds steady-state break in an array of data to permit calibration

clear;clc;
close all

% get file name
prompt = 'Enter file name (including file extension): ';
file = input(prompt, 's');
avgpts = input('Enter the points over which to average: ');
error = input('Enter the acceptable error: ');
% get data column (display headers?)
data = xlsread(file);
% col = 16;
col = input('Enter column number: ');
values = data(:,col);
% valuesavg rolling 10 sec avg of data

dvdt = ones(size(values));
dvdtavg = ones(size(values));
valuesavg = ones((length(values)-avgpts),1);

i = 2;

for i = 2:length(values)
    dvdt(i) = (values(i) - values(i-1))/((values(i)+values(i-1))/2);
    if i < avgpts
        dvdtavg(i) = dvdt(i);
    else
        dvdtavg(i) = mean(dvdt(i-(avgpts-1):i));
        valuesavg(i-avgpts+1) = mean(values((i-avgpts+1):i));
    end
end

devflip = flipud(dvdtavg);
devcheck = devflip(1);
countback = 1;

while abs(devcheck) < error
    devcheck = devflip(countback);
    countback = countback + 1;
end

avgval = mean(values((end-countback):end));
ssdev = std(values((end-countback):end));
sstime = length(values)-countback;

display(avgval)
display(ssdev)
display(sstime)
```



## Appendix G. ssoptions.m MATLAB script for deciding most effective choice of average and error to use for finding steady-state value for sensor calibration.

```

% ssoptions.m
% Evaluates multiple avg pts/error pct scenarios
% Validate method w/Excel

clear;clc;

prompt = 'Enter file name (including file extension): ';
file = input(prompt, 's');
data = xlsread(file);
avgpts = 10:5:50;
error = 0.001:0.001:0.01;
col = 1;
values = data(:,col);

dvdt = ones(size(values));
dvdtavg = ones(size(values));
% valuesavg = ones(size(values));

countback = ones(length(error),length(avgpts));
avgval = ones(length(error),length(avgpts));
ssdev = ones(length(error),length(avgpts));
sstime = ones(length(error),length(avgpts));

i = 1;
j = 1;
k = 2;

for i = 1:length(error)
    for j = 1:length(avgpts)
        for k = 2:length(values)
            dvdt(i,j,k) = (values(k) - values(k-1))/((values(k)+values(k-1))/2);
            if k < avgpts(j)
                dvdtavg(k) = dvdt(k);
            else
                dvdtavg(k) = mean(dvdt(i,j,(k-avgpts(j)+1):k));
                % valuesavg(k-avgpts(j)+1) = mean(values((k-avgpts(j)+1):k));
            end
        end
        % Don't need to save dvdtavg values
        % Spit relevant info to array, move on/overwrite
        devflip = flip(dvdtavg);
        devcheck = devflip(1);
        while abs(devcheck) < error(i)
            devcheck = devflip(countback);
            countback(i,j) = countback(i,j) + 1;
        end
        avgval(i,j) = mean(values((end-countback(i,j)):end));
        ssdev(i,j) = std(values((end-countback(i,j)):end));
        sstime(i,j) = length(values)-countback(i,j);
    end
end
end

```

## Appendix H. slopefind.m MATLAB script for original attempts at fitting a curve to the IR CO<sub>2</sub> data and calculating initial emission rate.

```

% slopefind

% Get initial slope of concentration curve to infer gas production rate via
% Fick's First Law of diffusion
clear;clc;

prompt = 'Enter the file name including path & extension. ';
file = input(prompt, 's');
IRdata = xlsread(file,'IRavg');
% GCdata = xlsread(file,'GCsum');
% t = GCdata(:,1);
% co2GC = GCdata(:,2);
% co2GCstd = GCdata(:,3);

time = IRdata(:,1);
conc = IRdata(:,2);

co2IR = [conc(1),conc(500),conc(1000),conc(1500)];

V = 5.4; % chamber volume, liters
A = .05; % chamber footprint, m^2
P = 101325; % pressure, Pa
T = 303; % ambient temp at start, K - need actual temp
R = 188.9; % J/(kg*K)

f1 = fit(time,conc,'fourier2');
[df1] = differentiate(f1,time);

% df2 = ((co2GC(2)-co2GC(1))^2)/(500*(2*co2GC(2)-co2GC(3)-co2GC(1)))*log((co2GC(2)-
co2GC(1))/(co2GC(3)-co2GC(2)));

IR4pt = ((co2IR(2)-co2IR(1))^2)/(500*(2*co2IR(2)-co2IR(3)-co2IR(1)))*log((co2IR(2)-
co2IR(1))/(co2IR(3)-co2IR(2)));

rate1 = df1(1)*V*P*(10^-6)/(R*T*A*(1/3600)); % g/(m^2*hr)
% rate2 = df2(1)*V*P*(10^-6)/(R*T*A*(1/3600)); % g/(m^2*hr)

figure()
plot(f1,time,conc)

display(rate1)
% display(rate2)

```

## BIBLIOGRAPHY

- Amon, B., Amon, T., Boxberger, J., & Alt, C. (2001). Emissions of NH<sub>3</sub>, N<sub>2</sub>O and CH<sub>4</sub> from dairy cows housed in a farmyard manure tying stall (housing, manure storage, manure spreading). *Nutrient Cycling in Agroecosystems*, 60(1-3), 103-113. doi: 10.1023/A:1012649028772
- Bain, W. G., Hutyra, L., Patterson, D. C., Bright, A. V., Daube, B. C., Munger, J. W., & Wofsy, S. C. (2005). Wind-induced error in the measurement of soil respiration using closed dynamic chambers. *Agricultural and Forest Meteorology*, 131(3-4), 225-232. doi: <http://dx.doi.org/10.1016/j.agrformet.2005.06.004>
- Berman, A. (2005). Estimates of heat stress relief needs for Holstein dairy cows. *Journal of animal science*, 83(6), 1377-1384.
- Bewley, J., Taraba, J., Day, G., & Black, R. (2012). Compost bedded pack barn design features and management considerations. *Cooperative Extension Publ. ID-206, Cooperative Extension Service, University of Kentucky College of Agriculture, Lexington KY.*
- Black, R., Bewley, J., Taraba, J., Day, G., & Damasceno, F. (2013). Kentucky compost-bedded pack barn project. *Cooperative extension service, University of Kentucky, College of agriculture, Lexington, KY, USA.*
- Black, R. A. (2013). Compost Bedded Pack Barns: Management Practices and Economic Implications.
- Black, R. A., Taraba, J. L., Day, G. B., Damasceno, F. A., & Bewley, J. M. (2013). Compost bedded pack dairy barn management, performance, and producer satisfaction. *Journal of Dairy Science*, 96(12), 8060-8074. doi: 10.3168/jds.2013-6778
- Black, R. A., Taraba, J. L., Day, G. B., Damasceno, F. A., Newman, M. C., Akers, K. A., . . . Bewley, J. M. (2014). The relationship between compost bedded pack performance, management, and bacterial counts. *J Dairy Sci*, 97(5), 2669-2679. doi: 10.3168/jds.2013-6779
- Bonifacio, H. F., Rotz, C. A., Leytem, A. B., Waldrip, H. M., & Todd, R. W. (2015). Process-based modeling of ammonia and nitrous oxide emissions from open-lot beef and dairy facilities. *Transactions of the ASABE*, 58(3), 827-846.
- Brewer, S., & Costello, T. (1999). In situ measurement of ammonia volatilization from broiler litter using an enclosed air chamber. *Transactions of the ASAE*, 42(5), 1415-1422.
- Cabezas-Garcia, E., Krizsan, S., Shingfield, K., & Huhtanen, P. (2017). Between-cow variation in digestion and rumen fermentation variables associated with methane production. *Journal of Dairy Science*.
- Christiansen, J. R., Korhonen, J. F., Juszczak, R., Giebels, M., & Pihlatie, M. (2011). Assessing the effects of chamber placement, manual sampling and headspace mixing on CH<sub>4</sub> fluxes in a laboratory experiment. *Plant and soil*, 343(1-2), 171-185.
- Conen, F., & Smith, K. A. (1998). A re-examination of closed flux chamber methods for the measurement of trace gas emissions from soils to the atmosphere. *European Journal of Soil Science*, 49(4), 701-707. doi: 10.1046/j.1365-2389.1998.4940701.x

- Davidson, E. A., Savage, K., Verchot, L. V., & Navarro, R. (2002). Minimizing artifacts and biases in chamber-based measurements of soil respiration. *Agricultural and Forest Meteorology*, *113*(1-4), 21-37. doi: [http://dx.doi.org/10.1016/S0168-1923\(02\)00100-4](http://dx.doi.org/10.1016/S0168-1923(02)00100-4)
- Eckelkamp, E., Taraba, J., Akers, K., Harmon, R., & Bewley, J. (2016). Understanding compost bedded pack barns: Interactions among environmental factors, bedding characteristics, and udder health. *Livestock Science*, *190*, 35-42.
- Eckelkamp, E. A. (2014). Compost Bedded Pack Barns for Dairy Cattle: Bedding Performance and Mastitis as Compared to Sand Freestalls.
- Ferguson, N., Gates, R., Taraba, J., Cantor, A., Pescatore, A., Straw, M., . . . Burnham, D. (1998). The effect of dietary protein and phosphorus on ammonia concentration and litter composition in broilers. *Poultry Science*, *77*(8), 1085-1093.
- Galama, P., de Boer, H., van Dooren, H., Ouweltjes, W., & Driehuis, K. (2015). Sustainability aspects of ten bedded pack dairy barns in The Netherlands: Wageningen UR Livestock Research.
- Gates, R., Taraba, J., Ferguson, N., & Turner, L. (1997). A technique for determining ammonia equilibrium and volatilization from broiler litter. ASAE Intl. Meeting, August 10-14, Minneapolis: MN. ASAE Paper.
- Gill, M., Smith, P., & Wilkinson, J. (2010). Mitigating climate change: the role of domestic livestock. *animal*, *4*(03), 323-333.
- Gourley, C. J. P., Aarons, S. R., & Powell, J. M. (2012). Nitrogen use efficiency and manure management practices in contrasting dairy production systems. *Agriculture, Ecosystems & Environment*, *147*, 73-81. doi: [10.1016/j.agee.2011.05.011](https://doi.org/10.1016/j.agee.2011.05.011)
- Hammond, L. (2015). Nutrient Availability and Dynamics of Compost Bedded Pack Dairy Barn Waste.
- Hutchinson, G., & Livingston, G. (2001). Vents and seals in non-steady-state chambers used for measuring gas exchange between soil and the atmosphere. *European Journal of Soil Science*, *52*(4), 675-682.
- Hutchinson, G., & Mosier, A. (1981). Improved soil cover method for field measurement of nitrous oxide fluxes. *Soil Science Society of America Journal*, *45*(2), 311-316.
- Huxley, J. (2013). Impact of lameness and claw lesions in cows on health and production. *Livestock Science*, *156*(1), 64-70.
- Janni, K., Endres, M., Reneau, J., & Schoper, W. (2007). Compost dairy barn layout and management recommendations. *Applied engineering in agriculture*, *23*(1), 97.
- Jensen, L. S., Mueller, T., Tate, K. R., Ross, D. J., Magid, J., & Nielsen, N. E. (1996). Soil surface CO<sub>2</sub> flux as an index of soil respiration in situ: A comparison of two chamber methods. *Soil Biology and Biochemistry*, *28*(10-11), 1297-1306. doi: [http://dx.doi.org/10.1016/S0038-0717\(96\)00136-8](http://dx.doi.org/10.1016/S0038-0717(96)00136-8)
- Kentucky Farm Bureau. (2015). Commodity Booklet.
- Klaas, I. C., Bjerg, B. S., Friedmann, S., & Bar, D. (2010). Cultivated barns for dairy cows: an option to promote cattle welfare and environmental protection in Denmark? *Dansk Veterinærtidsskrift*, *93*(9), 20-29.
- Knapp, J., Laur, G., Vadas, P., Weiss, W., & Tricarico, J. (2014). Invited review: Enteric methane in dairy cattle production: Quantifying the opportunities and impact of reducing emissions. *Journal of Dairy Science*, *97*(6), 3231-3261.

- Kremen, A., Bear, J., Shavit, U., & Shaviv, A. (2005). Model demonstrating the potential for coupled nitrification denitrification in soil aggregates. *Environmental science & technology*, 39(11), 4180-4188.
- Leytem, A. B., Dungan, R. S., Bjorneberg, D. L., & Koehn, A. C. (2011). Emissions of ammonia, methane, carbon dioxide, and nitrous oxide from dairy cattle housing and manure management systems. *J Environ Qual*, 40(5), 1383-1394.
- Li, X., & Group, A. A. R. U. (2000). *Evaluation of methods for determining NH<sub>3</sub> and N<sub>2</sub>O emissions from soil applied manure*: Air Research Users Group, Alberta Environment.
- Liang, D., Sun, F., Wattiaux, M., Cabrera, V., Hedtcke, J., & Silva, E. (2017). Effect of feeding strategies and cropping systems on greenhouse gas emission from Wisconsin certified organic dairy farms. *Journal of Dairy Science*.
- Maia, G., Sales, G., Gates, R., & Taraba, J. (2012). Characterizing physical properties of gas-phase biofilter media. *Transactions of the ASABE*, 55(5), 1939-1950.
- Maia, G. D. N. (2010). *Ammonia biofiltration and nitrous oxide generation as affected by media moisture content*. University of Kentucky.
- McDowell, R. W. (2008). *Environmental impacts of pasture-based farming*: CABI.
- Mujumdar, A. S., & Menon, A. S. (1995). Drying of solids: principles, classification, and selection of dryers. *Handbook of industrial drying, 1*, 1-39.
- Njuki, E., & Bravo-Ureta, B. E. (2015). The Economic Costs of Environmental Regulation in U.S. Dairy Farming: A Directional Distance Function Approach. *American Journal of Agricultural Economics*, 97(4), 1087-1106. doi: 10.1093/ajae/aav007
- Parkin, T. B., & Venterea, R. T. (2010). USDA-ARS GRACEnet project protocols, chapter 3. Chamber-based trace gas flux measurements. *Sampling protocols. Beltsville, MD p*, 1-39.
- Parkin, T. B., Venterea, R. T., & Hargreaves, S. K. (2012). Calculating the detection limits of chamber-based soil greenhouse gas flux measurements. *J Environ Qual*, 41(3), 705-715. doi: 10.2134/jeq2011.0394
- Paul, E. A. (2014). *Soil microbiology, ecology and biochemistry*: Academic press.
- Pumpanen, J., Kolari, P., Ilvesniemi, H., Minkinen, K., Vesala, T., Niinistö, S., . . . Hari, P. (2004). Comparison of different chamber techniques for measuring soil CO<sub>2</sub> efflux. *Agricultural and Forest Meteorology*, 123(3-4), 159-176. doi: <http://dx.doi.org/10.1016/j.agrformet.2003.12.001>
- Sexstone, A. J., Revsbech, N. P., Parkin, T. B., & Tiedje, J. M. (1985). Direct measurement of oxygen profiles and denitrification rates in soil aggregates. *Soil Science Society of America Journal*, 49(3), 645-651.
- SGX (2010). Infrared Sensor Application Note 2: Signal Processing for Infrared Gas Sensors. Retrieved from <https://www.sgxsensortech.com/content/uploads/2014/08/AN2-%E2%80%93Signal-Processing-for-Infrared-Gas-Sensors.pdf>
- Shane, E., Endres, M., & Janni, K. (2010). Alternative bedding materials for compost bedded pack barns in Minnesota: a descriptive study. *Applied engineering in agriculture*, 26(3), 465-473.
- Sylvia, D. M., Fuhrmann, J. J., Hartel, P. G., & Zuberer, D. A. (2005). *Principles and applications of soil microbiology*: Pearson Prentice Hall Upper Saddle River, NJ:.

- Thoma, G., Popp, J., Nutter, D., Shonnard, D., Ulrich, R., Matlock, M., . . . East, C. (2013). Greenhouse gas emissions from milk production and consumption in the United States: A cradle-to-grave life cycle assessment circa 2008. *International Dairy Journal*, 31, S3-S14.
- Umetsu, K., Kimura, Y., Takahashi, J., Kishimoto, T., Kojima, T., & Young, B. (2005). Methane emission from stored dairy manure slurry and slurry after digestion by methane digester. *Animal Science Journal*, 76(1), 73-79. doi: 10.1111/j.1740-0929.2005.00240.x
- Wang, W., Chen, G., & Mujumdar, A. S. (2007). Physical interpretation of solids drying: An overview on mathematical modeling research. *Drying Technology*, 25(4), 659-668.
- Willits, D. H. (1974). *A mathematical drying model for manure based on the concept of a receding evaporative interface*: publisher not identified.
- Woodbury, B., Miller, D., Eigenberg, R., & Nienaber, J. (2006). Technical note: An inexpensive laboratory and field chamber for manure volatile gas flux analysis. *Transactions-American Society of Agricultural Engineers*, 49(3), 767.
- Xu, L., Furtaw, M. D., Madsen, R. A., Garcia, R. L., Anderson, D. J., & McDermitt, D. K. (2006). On maintaining pressure equilibrium between a soil CO<sub>2</sub> flux chamber and the ambient air. *Journal of Geophysical Research: Atmospheres*, 111(D8), n/a-n/a. doi: 10.1029/2005JD006435

## **VITA**

### **Place of birth**

Jacksonville, NC

### **Education**

B.S. 2015 University of Kentucky Biosystems and Agricultural Engineering

### **Professional Affiliations**

American Society of Agricultural and Biological Engineers

American Dairy Science Association

American Registry of Professional Animal Scientists

American Dairy Goat Association

Alpha Epsilon: The Honor Society of Agricultural, Food, and Biological Engineering